

# Early Paleozoic Back-Arc and Island-Arc Settings in Greenstone Sequences of the Central Tauern Window (Eastern Alps)

By WOLFGANG FRISCH & DIETER RAAB\*)

With 15 Figures and 4 Tables

Austria  
Tauern Window  
Lower Paleozoic  
Greenstones (amphibolites)  
Metamorphism  
Geochemistry  
Back-arc basin  
Island arc

Österreichische Karte 1 : 50.000  
Blatt 152

## Contents

|   |     |
|---|-----|
| Zusammenfassung                                 | 545 |
| Summary   | 545 |
| 1. Introduction                                 | 546 |
| 2. The Lithologic Units                         | 547 |
| 3. Metamorphism                                 | 550 |
| 4. Geochemistry                                 | 553 |
| 4.1. The Stubachtal Complex                     | 553 |
| 4.2. The Basis Amphibolite East of Felbertauern | 555 |
| 4.3. The Felbertal Mine Amphibolites            | 559 |
| 4.4. The Weinbühel Amphibolite                  | 559 |
| 4.5. The Tauernkogel Amphibolite                | 561 |
| 5. Discussion and Conclusions                   | 564 |
| Acknowledgements                                | 565 |
| References                                      | 565 |

### Zusammenfassung

Im zentralen Teil des Tauernfensters wurden Grünsteinfolgen (hauptsächlich niedriggradige Amphibolite) petrographisch und geochemisch untersucht. Ihr vermutetes Alter, das in einem Fall auch radiometrisch belegt ist, ist frühpaläozoisch.

Der Basisamphibolitkomplex enthält ultramafische Gesteine (z. B. Stubachtal) und metagabbroische und metabasaltische Amphibolite. Die alpidische Metamorphose hat bereichsweise vermutlich die Grenze zur Amphibolitfazies überschritten. Der geochemische Charakter der Metabasite wird einem Bildungsmilieu im Backarc-Bereich hinter einem Inselbogen zugeschrieben. Es gibt auffallende Ähnlichkeiten zur Geotimes-Einheit in Oman.

Der Weinbühel- und der Tauernkogelamphibolit, die beide der Habachformation angehören (der Tauernkogelamphibolit ist Teil der Riffldecke), zeigen mit ihren zoniert gebauten Plagioklasen und Amphibolen prograde Metamorphose bis in die höhere Grünschieferfazies an. Die Ausgangsgesteine waren hauptsächlich Andesite mit low-K-Charakter, doch gibt es auch Basalte und Dazite. Aufgrund ihrer geochemischen Zusammensetzung können die Gesteine als typische primitive Inselbogenfolge klassifiziert werden. Stark deformierte und rekristallisierte Gesteine enthalten infolge passiver Anreicherung erhöhte Konzentrationen von immobilen Spurenelementen. Ihr sekundäres Spurenelementmuster ähnelt daher jenem alkalischer Gesteine. Metasedimentgesteine sind großteils vulkano-detritischen Ursprungs.

Die Amphibolite der Scheelitlagerstätte Felbertal gehören der Habachformation an (Fortsetzung des Weinbühelamphibolits), weisen aber geochemische Charakteristika auf, die an die Backarc-Sequenz des Basisamphibolits erinnern. Möglicherweise repräsentieren sie ein Übergangsstadium zwischen der Bildung des Backarc-Beckens und des Inselbogens der Habachformation, die auf der Backarc-Kruste aufsetzt.

Die Amphibolitfolgen werden von variszischen Granitoiden intrudiert oder tektonisch unterlagert, die durch die alpidische Gebirgsbildung zu den meist längsgestreckten Zentralgneiskörpern umgeformt wurden. Die Situation erinnert an archaische Granit-Grünstein-Gürtel, für deren Bildung verschiedentlich ein Backarc-Milieu gefordert wurde.

### Summary

In the central part of the Tauern Window, greenstone sequences (mainly low grade amphibolites) of an inferred and, in one case, proven, early Paleozoic age were investigated petrographically and geochemically.

The Basis Amphibolite Complex contains ultramafic rocks (Stubachtal Body) and metagabbroic and metabasaltic amphibolites. Alpine metamorphism is suggested to have reached the medium-grade level in places. The geochemical character of the metabasic rocks is interpreted in terms of a back-arc geotectonic setting behind an island arc. There are striking similarities to the Geotimes unit in Oman.

The Weinbühel and Tauernkogel Amphibolites, which belong to the Habach Formation (the Tauernkogel Amphibolite is part of the Riffl Nappe), show prograde metamorphism up to the upper greenschist facies on the base of zonation of plagioclase and amphibole. The source rocks are mainly andesites of low-K character but there are also basalts and dacites. From their geochemistry the rocks can be classified as a typical primitive island arc sequence. Strongly deformed and re-

\*) Authors' addresses: Univ.-Prof. Dr. WOLFGANG FRISCH, Institut für Geologie und Paläontologie, Universität Tübingen, Sigwartstraße 10, D-7400 Tübingen; DIETER RAAB, Institut für Gewässerschutz und Wassertechnologie der ETH, Überlandstraße 133, CH-8600 Dübendorf.

crystallised rocks contain elevated levels of immobile trace elements due to passive enrichment. They therefore attained a secondary trace element pattern similar to that of alkaline rocks. Metasedimentary rocks are mainly of volcano-detrital origin.

The amphibolites of the Felbertal scheelite mine belong to the Habach Formation (continuation of the Weinbühel Amphibolite) but show a geochemical pattern reminiscent of the back-arc sequence of the Basis Amphibolite. They possibly represent a transitional stage between the formation of the back-arc basin and the island arc of the Habach Formation which formed on top of the back-arc crust.

Variscan granitoids are found as intrusions in the amphibolite sequence or underlie the sequences with tectonic contacts. These granitoids were altered to the generally elongate Zentralgneis bodies during Alpidic times. The overall situation resembles Archaean granite-greenstone belts, for which a back-arc setting has been proposed by several authors.

# 1. Introduction

The area around Felbertauern, a nearly 2500 m high mountain pass between the Venediger massif to the W and the Granatspitz massif to the E, yields an excellent profile through the pre-Zentralgneis series within the Tauern window (Fig. 1). These series consist mainly of metabasites and are part of the Middle Penninic basement of the Venediger nappe. They have an inferred lower Paleozoic age (CORNELIUS & CLAR, 1939; FRASL, 1958). Recent U/Pb dating on zircon from the Felbertal schellite mine yielded an age of 500 Ma which is interpreted as the age of magmatic emplacement of the mafic and ultramafic rocks from which the zircon was separated (v. QUADT, 1985).

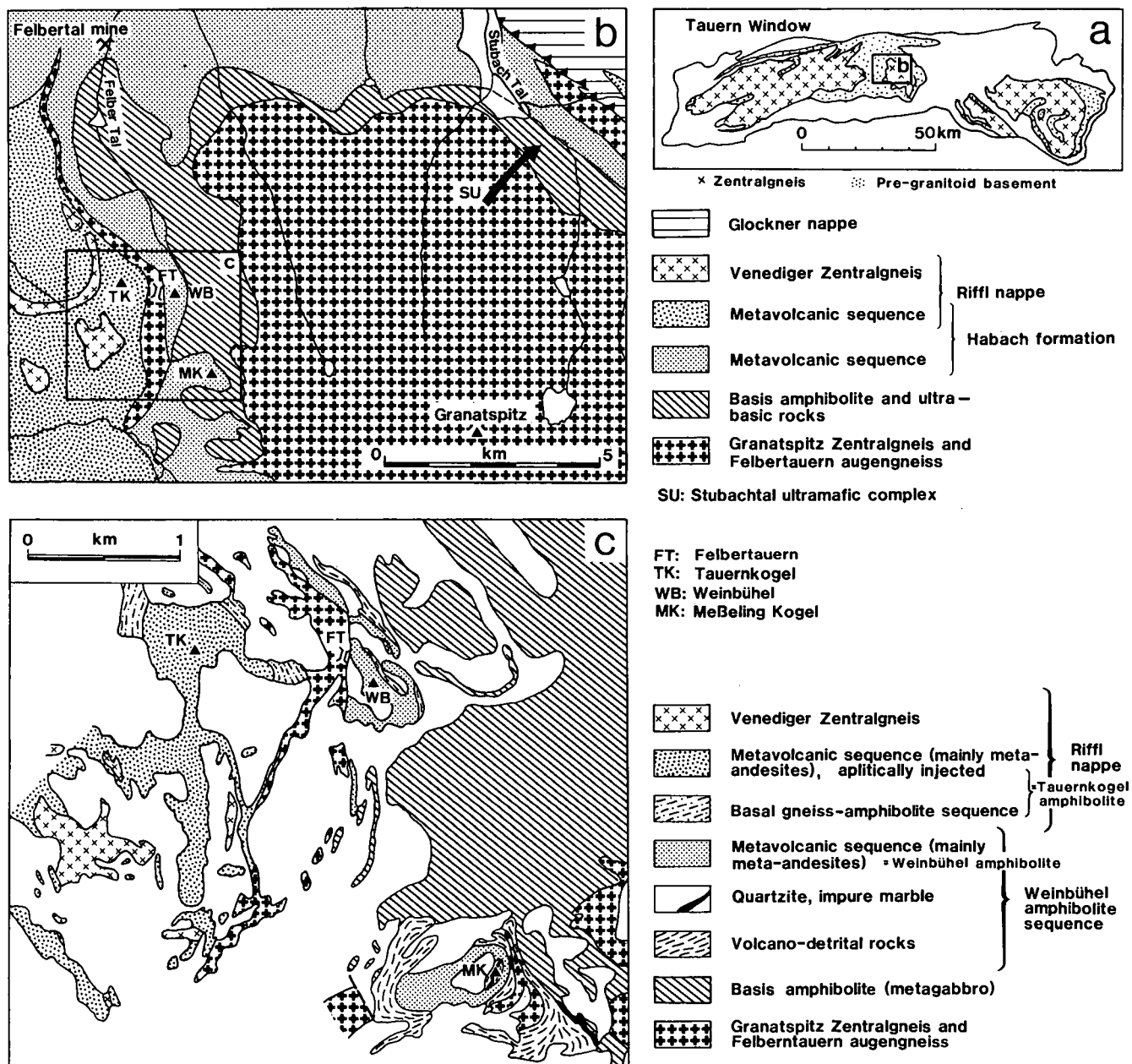


Fig. 1: Geological situation of the studied area.

- a) Sketch showing Zentralgneis (Hercynian granitoids) and Early Paleozoic sequences, both forming the basement complex of the Venediger nappe, which is the lower mega-unit in the Tauern Window.
- b) Map after FRASL & FRANK (1966) showing the sampled localities.
- c) Map after RAAB (1983) showing the situation around Felbertauern mountain pass in more detail.

The Zentralgneis represents Variscan granitoids which either intruded into the pre-existing series or came into tectonic contact with them during the Variscan or Alpidic orogenies. In the area concerned, the pre-granitoid series are in contact along tectonic boundaries with the Granatspitz Zentralgneis east of the Felbertauern. There are, however, intrusive relationships between the Venediger Zentralgneis and the Tauernkogel complex (Riffl Nappe) west of the Felbertauern as is indicated by the penetration of aplitic dike swarms (see Fig. 1).

The pre-granitoid series around Felbertauern are mainly made up of metabasic rocks, which have been metamorphosed to amphibolites. Gneisses representing dacitic tuffs and tuffites or their detrital derivatives are intercalated. Metasedimentary rocks of non-volcanic derivation are extremely rare and are restricted to layers of quartzite, graphitic quartzite, and impure marble.

Table 1 shows the lithostratigraphic units for the Felbertauern area after FUCHS (1958) and FRASL & FRANK (1966). CORNELIUS (1941) separated the Riffl Nappe, with its aplitic injections, and which is in primary contact with the Venediger Zentralgneis, from the underlying unit consisting of the Granatspitz Zentralgneis and its pre-existing envelope. CORNELIUS (1941) and FUCHS (1958) attributed a Triassic age to the quartzites and marbles and considered them a tectonic slice. FRISCH (1977, 1980) showed that these rocks belong to the Paleozoic assemblage. FRISCH (1980) and RAAB (1983) re-established the original concept of CORNELIUS of one Riffl Nappe, which had been modified by FUCHS (1958; see Table 1). A Variscan age was proposed for this nappe.

The envelope of the Granatspitz Zentralgneis beneath the Riffl Nappe and in the area of Hollersbach Tal and Habach Tal to the northwest, have been termed the "Habachserie" by FRASL (1958). He considers this succession, which is rich in basic volcanics, but also contains intermediate to acid volcanics and important volumes of black schists with minor quartzites etc., to be an early Paleozoic "geosynclinal filling". FRASL & FRANK (1966) drew a parallel between the Weinbühel Amphibolite and Habachserie.

In recent times, after the important find of the Felbertal scheelite deposit, HÖLL (1975) investigated the amphibolite sequences in detail and proposed a plate tectonic model for the Lower Paleozoic (HÖLL & MAUCHER, 1976). In this model the volcanic sequences of the Tauern Window are placed in a back-arc situation above a subduction zone. STEYRER (1983), who investigated the Habach Formation near the northern margin of the Tauern Window (Habach Tal, Untersulzbach Tal), proposed a tectonic setting in the magmatic arc of an active continental margin and took the Andes as an example. PESTAL (1983) considered an island arc in connection with a Caledonian geosyncline.

The present study aims to clarify the controversially interpreted tectonic setting of the volcanic sequences. Field work was carried out in the Felbertauern region (Fig. 1). Samples were also taken from the Stubachtal ultramafic/mafic body which is part of the Basis (basal) Amphibolite (CORNELIUS & CLAR, 1939; FRASL & FRANK, 1966), and from the Felbertal tungsten mine. In the Felbertauern section a distinction has been made between the Basis Amphibolite, the Weinbühel Amphibolite and the Tauernkogel Amphibolite, the latter representing the injected amphibolites above the Felbertauern Augengneiss (Fig. 1).

## 2. The Lithologic Units

In the Felbertauern section the lithological units, which are tectonically dismembered, have the following features:

- 1) The Basis Amphibolite represents a metagabbroic complex. In other sections the Basis Amphibolite is represented by metabasaltic and ultramafic rocks (e. g. Stubachtal).
- 2) The mainly amphibolitic complex of Weinbühel and Messelingkogel is a predominantly metavolcanic sequence with minor amounts of metasediments. Meta-andesites predominate.
- 3) The largely amphibolitic complex of Tauernkogel, which also contains important volumes of gneisses, is part of the Riffl nappe and is characterised by ap-

Table 1: Geological concepts for the Felbertauern section between the Granatspitz and Venediger Zentralgneis complexes. Compare Fig. 1.

| FUCHS (1958)  |              | FRASL & FRANK (1966)            |              | THIS PAPER  |             | AGE                      |
|---|--------------|---------------------------------|--------------|---|-------------|--------------------------|
| Venediger Zentralgneis                                  | Riffl nappes | Venediger Zentralgneis          | Riffl nappes | Venediger Zentralgneis  | Riffl nappe | C**                      |
| Aplitically injected amphibolites, gneisses and schists |              | Serie der Alten Gneise (PG-G ?) |              | Tauernkogel amphibolite* sequence                               |             | Pz1                      |
| Felbertauern augengneiss                                |              | Felbertauern augengneiss        |              | Felbertauern augengneiss  |             | C                        |
| Weinbühel amphibolite                                   |              | Habachserie (O-D, C1 ?)         |              | Weinbühel amphibolite* sequence including metasedimentary rocks |             | Pz1**<br>500Ma<br>(mine) |
| Metasedimentary layer (in part Triassic)                |              |                                 |              |   |             |                          |
| Basis amphibolite                                       |              | Amphibolitfolge (O-D, C1 ?)     |              | Basis amphibolite   |             | Pz1                      |
| Granatspitz Zentralgneis                                |              | Granatspitz Zentralgneis        |              | Granatspitz Zentralgneis  |             | C**                      |

\* Weinbühel and Tauernkogel amphibolite are part of the Habach formation.

\*\* Radiometric age. Other ages inferred.

PG, Precambrian. Pz1, Early Paleozoic. G, Cambrian. O, Ordovician. D, Devonian. C, Carboniferous. C1, Lower Carboniferous.

litic dike swarms deriving from the Venediger Zentralgneis. It otherwise corresponds to the Weinbühel amphibolite.

We consider the Basis Amphibolite and the accompanying ultrabasic rocks as one sequence, and the Weinbühel and Tauernkogel assemblages as a separate sequence (Habach Formation) of a different genetic origin, which was deposited upon the Basis Amphibolite.

The Basis Amphibolite rests upon the Granatspitz Zentralgneis and is separated from it by a pronounced shear horizon. Generally, it shows the coarse texture of gabbro though it is strongly deformed and recrystallized. In shear zones the typical flaser structure is replaced by a fine lamination of hornblende-rich and plagioclase-rich layers (Fig. 2a, b). Isoclinal folding of this layering implies a complex but not necessarily polyphase history for the rock. Crosscutting plagioclase veins are present. Hornblenditic lenses or nodules, which might be thought to represent original pyroxene cumulates, are better interpreted as metamorphic differentiates. Primary differences in the pyroxene/plagioclase ratio, however, cannot be ruled out. As a whole, the Basis Amphibolite represents a rather homogenous body. The microfabric is nearly completely recrystallised under high greenschist to lowest amphibolite facies conditions. The rock consists mainly of hornblende and plagioclase. There are no relics of polysynthetically twinned magmatic plagioclase. Some outstanding, large hornblende crystals may represent the shape relics of former pyroxene crystals. Their length/width ratio is much lower than that of the granoblastic hornblende. In rare cases relict orthopyroxene crystals are preserved; these are enstatites with marked zoning and clearcut narrow rims, which are richer in iron than the cores. Since orthopyroxene is uncommon in basic volcanic rocks (DEER, HOWIE & ZUSSMAN, 1963; EWART, 1982), the plutonic character of this rock body is supported.

In some places, the Basis Amphibolite is accompanied by ultramafic rocks. The most famous locality is the Stubachtal ultramafic body at the northeastern margin of the Granatspitz Zentralgneis (Fig. 1). The sampled rocks comprise dunites, serpentinised harzburgites, lherzolites, websterites and clinopyroxenites. PETRAKAKIS (1977) also reports wehrlite. Near Matreier Tauernhaus south of Felbertauern, CORNELIUS (1941) and FUCHS (1958) reported a lens of 10 m length of serpentinite situated within the Basis Amphibolite. FRISCH (1970) described serpentinite of dunitic composition and diopsidic pyroxenite from the underground section of the Felbertauern road tunnel from near the bottom of the amphibolite sequence.

The rocks of the Felbertal tungsten mine, which were sampled in the underground west field, are a lateral continuation of the Weinbühel Amphibolite. The sampled rocks, however, have mainly basaltic composition and show by their chemistry close relationship to the metabasalts of the Basis Amphibolite (see Section 4). Mobilisation of plagioclase and quartz in veins and passive enrichment of amphibole and sphene in clusters and layers led to the formation of hornblende-rich and hornblenditic rocks.

The Weinbühel Complex is mainly made up of amphibolites and contains plagioclase gneisses to minor extents. The basal layer of metasedimentary

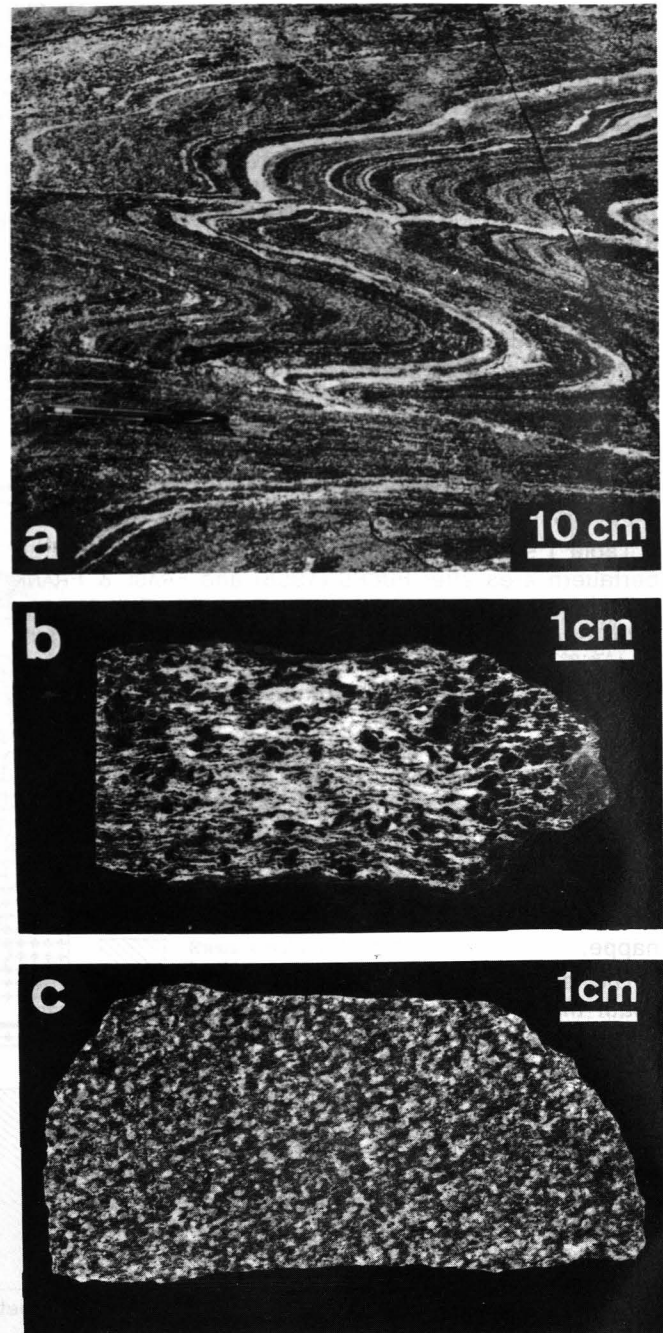


Fig. 2

- Strongly sheared and folded gabbroic Basis Amphibolite, east of Felbertauern. The banding is caused by metamorphic differentiation.
- Gabbroic Basis Amphibolite showing flaser structure. Sample 2333 NW of Messelingkogel.
- Andesitic Weinbühel Amphibolite with knotty structure caused by intense plagioclase blastesis, which outlasted deformation. Sample 2320, north-western foot of Messelingkogel.

rocks east of Weinbühel is in tectonic contact with the underlying Basis Amphibolite and is part of the Weinbühel succession. The prevailing biotite schists are made up of the same minerals as the metavolcanic rocks, i. e. plagioclase, hornblende, biotite, quartz, epidote, chlorite, and sphene are the more important phases. The proportions, however, are different. In particular there is remarkably less biotite and little or no quartz in the basic metavolcanic rocks. The biotite schists lack white mica and alkali feldspar. The trace element pattern is also comparable with that of the metavolcanic rocks. It is therefore concluded that these

rocks are the immediate detrital derivatives of the metavolcanics. Graphitic quartzites (e. g. near the southern entrance to the Felbertauern road tunnel or on Messelingkogel) indicate a depositional environment with reducing conditions. They are considered to represent metacherts.

Part of the Weinbühel Amphibolite is characterised by strong plagioclase blastesis, which gives the rock a knotty appearance ("prasinities" of Alpine literature) (Fig. 2c). Most of the amphibolites have the chemical composition of andesites but sometimes also that of dacites and only very subordinate of basalts. Rocks of different composition form banded sequences in places. Intercalated acidic gneisses are rich in plagioclase, quartz, and white mica but are devoid of alkali feldspar. They contain epidote, chlorite, and amphibole. They represent tuffites or volcano-detrital rocks. Rounded zircon crystals with high elongation values point towards a volcano-detrital component.

The rocks of the Tauernkogel Complex (Riffl Nappe) on top of the Felbertauern Augengneiss are in principle the same as those of the Weinbühel although gneisses (again plagioclase gneisses of volcano-detrital or tuffitic origin) are more emphasised. The main differ-

ence between this complex and the Weinbühel Complex are the dike swarms transecting the succession. Near the Venediger Zentralgneiss narrowly spaced, s-parallel dikes may give the rock a migmatitic appearance. In regions which are more distant from the Zentralgneiss, the aplitic dikes become less frequent. So, for instance, the basal part of the Tauernkogel sequence west of Felbertauern does not contain dikes (Fig. 1).

There is no doubt that the amphibolites and gneisses of the Riffl Nappe are the equivalent of the Habach Formation. The Tauernkogel Complex is separated from the Weinbühel Complex by the Riffl Nappe thrust plane and the Felbertauern Augengneiss, which is probably a splinter of the Granatspitz or Habach Zentralgneiss.

Banded amphibolites form a distinct horizon in the Tauernkogel area. This rock type is characterised by an alternation of amphibolites and plagioclase gneiss layers of cm- to dm-thickness. The source rocks were andesitic tuffs alternating with dacitic tuff layers.

In both the Weinbühel and the Tauernkogel Complexes garnet amphibolites form rare intercalations. The amphiboles of these rocks are of dark green colour in thin section.

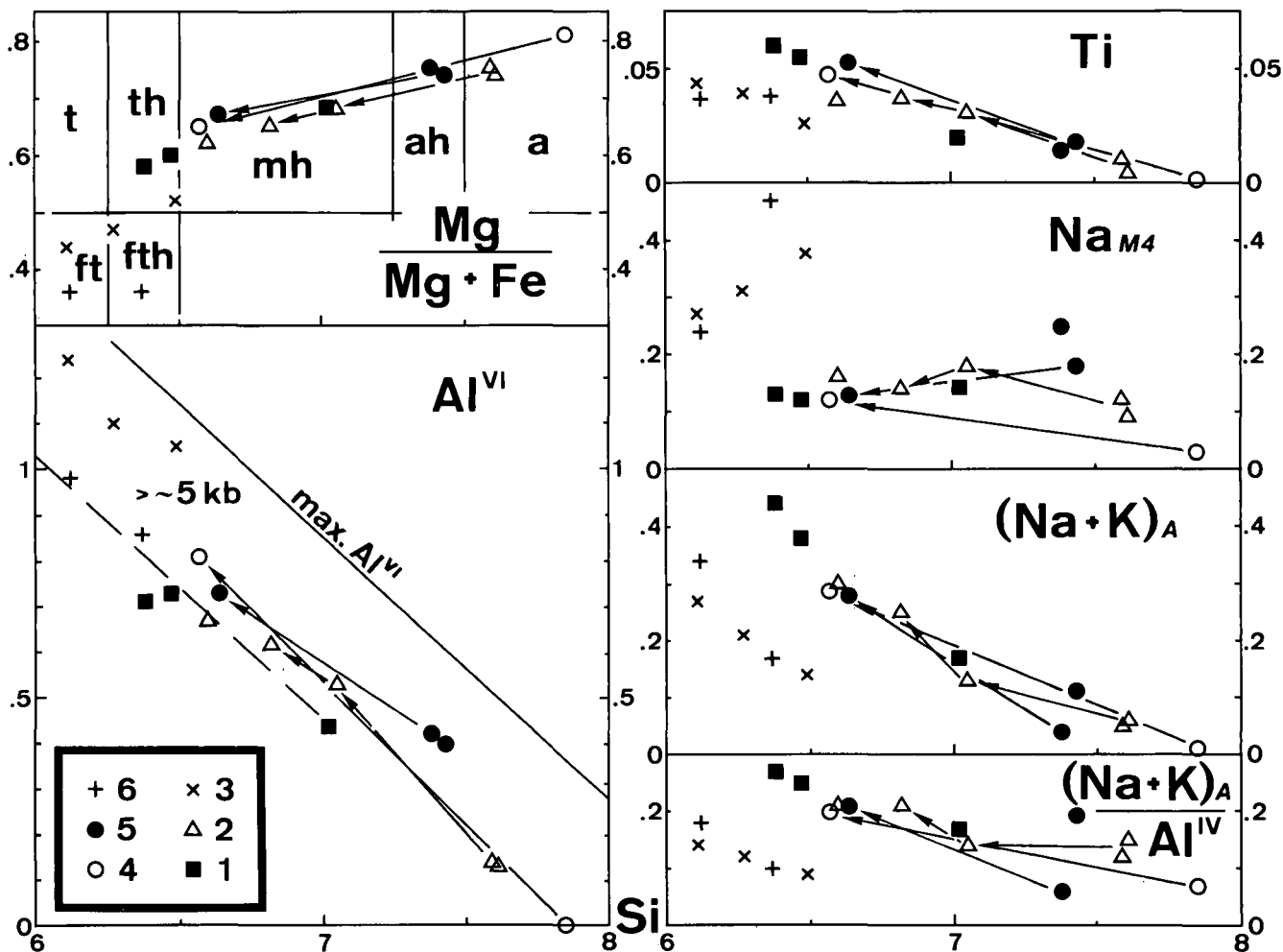


Fig. 3: Diagrams showing compositional variation of amphiboles. Upper left diagram shows nomenclature after LEAKE (1978). a = actinolite; ah = actinolitic hornblende; mh = magnesio-hornblende; th = tschermakitic hornblende; ft = ferro-tschermakite. Lower left diagram shows limit of maximal possible  $Al^{VI}$  (LEAKE, 1965) and field of amphiboles stable at pressures  $> \sim 5$  kb after RAASE (1974). Tie lines connect cores and rims of single crystals; the arrows point towards the rims. Symbols: 1 = Basis Amphibolite east of Felbertauern; 2,3 = Weinbühel Amphibolite (3 = garnet amphibolite); 4,5,6 = Tauernkogel Amphibolite (4 = basal sequence, 6 = garnet amphibolite).

### 3. Metamorphism

The grade of metamorphism can be best determined using the amphibolites. In the Felbertauern section the Alpidic deformation and metamorphism caused nearly complete recrystallisation. No previous metamorphic event can be distinguished with confidence in the rocks studied, but there are some indications from other localities of an older event (see below). In the Felbertauern area the general mineral paragenesis reflecting the Alpidic maximum temperature, is oligoclase ( $An > 17$ ) + magnesio- or tschermakitic hornblende + epidote + chlorite  $\pm$  biotite  $\pm$  quartz  $\pm$  iron oxide + sphene. Temperatures between ca. 500 and 550°C are required (upper region of low grade metamorphism). Prograde zoning is common in the plagioclase and partly in the amphibole except in the Basis Amphibolite. Actinolitic cores are only present in large amphibole crystals and are small. Adjustment by diffusion is likely

to have replaced the originally larger actinolite cores. Plagioclase porphyroblasts show large albite cores and sharp boundaries to narrow oligoclase rims. The peristerite gap is well developed. Twinning is rare but the oligoclase crystals sometimes show polysynthetic pericline twinning. Deformation did not outlast the temperature maximum. This is shown by the generally well-annealed fabric.

The Basis Amphibolite east of Felbertauern does not or only weakly show this prograde zoning of minerals. Diffusion processes between rims and cores will have been facilitated by slightly higher maximum temperatures in the Basis Amphibolite so that only rarely diffuse albite and no actinolite cores are preserved. The abundances of epidote and chlorite decrease significantly from the overlying Weinbühel Amphibolite into the Basis Amphibolite. It is suggested that the border of the amphibolite facies has been reached or slightly overstepped.

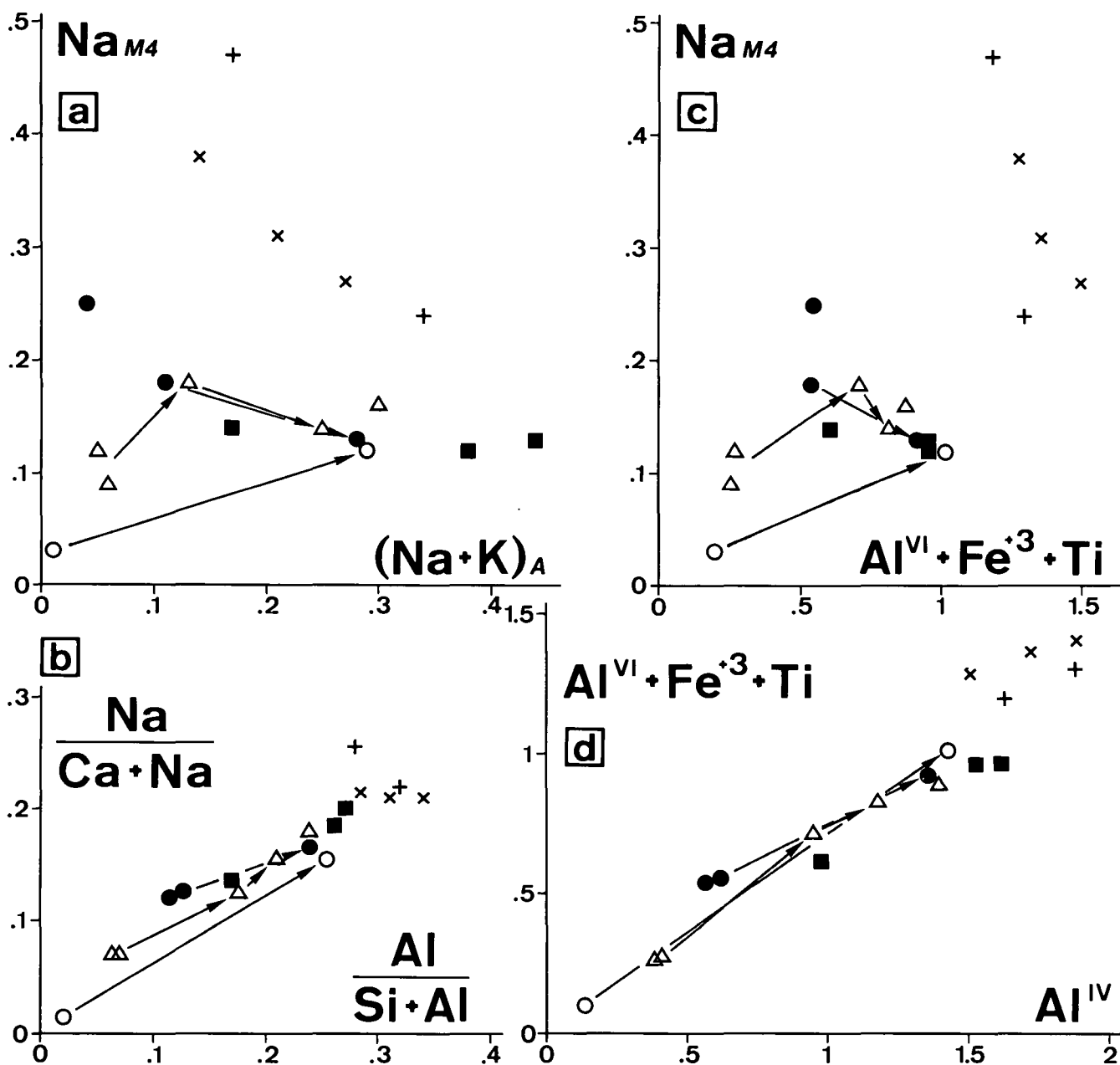


Fig. 4: Diagrams after LAEKE & ALBEE (1981) showing compositional variations of amphiboles. Parameters on abscissa in general indicate increasing temperature, those on ordinate increasing pressure.  $Fe^{3+}$  is taken as 0.1 Fe (see GRAHAM & POWELL, 1984). Symbols as in Fig. 3.

Table 2: Microprobe analyses of amphiboles from amphibolites of different settings.

Cation concentrations calculated on the basis of 23 oxygens. Symbols as in Fig. 3. C = cores, R = rims of zoned crystals. See diagrams in Figs. 3 and 4.

| Sample                         | ■ 1   | ■ 1   | ■ 1   | △ 2C  | △ 2C  | △ 2R  | △ 2R  | △ 2   | × 3   |
|--------------------------------|-------|-------|-------|-------|-------|-------|-------|-------|-------|
| SiO <sub>2</sub> %             | 47.41 | 43.58 | 42.55 | 52.46 | 52.60 | 49.21 | 46.71 | 44.76 | 44.36 |
| TiO <sub>2</sub>               | .18   | .49   | .53   | .03   | .10   | .28   | .34   | .33   | .24   |
| Al <sub>2</sub> O <sub>3</sub> | 8.16  | 12.92 | 13.21 | 3.07  | 3.22  | 8.77  | 10.46 | 11.92 | 14.88 |
| FeO                            | 12.33 | 14.17 | 14.89 | 10.45 | 10.30 | 12.44 | 12.92 | 13.98 | 16.40 |
| MgO                            | 14.48 | 11.96 | 11.53 | 17.17 | 17.36 | 14.75 | 13.43 | 12.75 | 10.14 |
| MnO                            | .23   | .30   | .23   | .18   | .18   | .12   | .21   | .15   | .28   |
| CaO                            | 11.72 | 11.80 | 11.68 | 12.30 | 12.15 | 11.85 | 11.87 | 11.67 | 10.34 |
| Na <sub>2</sub> O              | 1.01  | 1.49  | 1.61  | .49   | .49   | .95   | 1.20  | 1.39  | 1.57  |
| K <sub>2</sub> O               | .12   | .38   | .52   | .08   | .16   | .26   | .27   | .33   | .41   |
|                                | 95.64 | 97.09 | 96.75 | 96.23 | 96.56 | 98.63 | 97.41 | 97.28 | 98.62 |

|    |      |      |      |      |      |      |      |      |      |
|----|------|------|------|------|------|------|------|------|------|
| Si | 7.02 | 6.47 | 6.38 | 7.61 | 7.59 | 7.05 | 6.82 | 6.60 | 6.49 |
| Al | .98  | 1.53 | 1.62 | .39  | .41  | .95  | 1.18 | 1.40 | 1.51 |
| Al | .44  | .73  | .71  | .13  | .14  | .53  | .62  | .67  | 1.05 |
| Ti | .02  | .05  | .06  | .00  | .01  | .03  | .04  | .04  | .03  |
| Fe | 1.53 | 1.76 | 1.87 | 1.27 | 1.24 | 1.49 | 1.58 | 1.72 | 2.00 |
| Mn | .03  | .04  | .03  | .02  | .02  | .01  | .03  | .02  | .03  |
| Mg | 3.20 | 2.64 | 2.57 | 3.71 | 3.74 | 3.15 | 2.92 | 2.80 | 2.21 |
| Ca | 1.86 | 1.88 | 1.87 | 1.91 | 1.88 | 1.82 | 1.86 | 1.84 | 1.62 |
| Na | .14  | .12  | .13  | .09  | .12  | .18  | .14  | .16  | .38  |
| Na | .15  | .31  | .34  | .05  | .02  | .08  | .20  | .24  | .06  |
| K  | .02  | .07  | .10  | .01  | .03  | .05  | .05  | .06  | .08  |

|   |      |      |      |      |      |      |      |      |      |
|---|------|------|------|------|------|------|------|------|------|
| Y | 5.22 | 5.22 | 5.24 | 5.13 | 5.15 | 5.21 | 5.19 | 5.25 | 5.32 |
| A | .17  | .38  | .44  | .06  | .05  | .13  | .25  | .30  | .14  |

| Sample                         | × 3   | × 3   | ○ 4C  | ○ 4R  | ● 5C  | ● 5C  | ● 5R  | + 6   | + 6   |
|--------------------------------|-------|-------|-------|-------|-------|-------|-------|-------|-------|
| SiO <sub>2</sub> %             | 42.48 | 41.42 | 54.77 | 44.78 | 52.04 | 52.71 | 45.72 | 42.23 | 40.36 |
| TiO <sub>2</sub>               | .35   | .40   | .01   | .42   | .17   | .13   | .48   | .34   | .32   |
| Al <sub>2</sub> O <sub>3</sub> | 16.30 | 18.02 | .81   | 12.98 | 5.74  | 6.34  | 12.20 | 13.98 | 15.97 |
| FeO                            | 17.85 | 17.91 | 8.15  | 12.12 | 10.08 | 10.32 | 11.81 | 23.33 | 21.82 |
| MgO                            | 8.78  | 7.80  | 19.30 | 12.81 | 16.23 | 16.98 | 13.48 | 7.21  | 6.77  |
| MnO                            | .40   | .51   | .17   | .27   | .26   | .22   | .30   | .33   | .35   |
| CaO                            | 10.70 | 10.98 | 12.63 | 11.98 | 11.88 | 11.56 | 12.04 | 9.45  | 10.84 |
| Na <sub>2</sub> O              | 1.58  | 1.62  | .12   | 1.23  | .90   | .91   | 1.33  | 1.78  | 1.65  |
| K <sub>2</sub> O               | .35   | .41   | .06   | .32   | .21   | .20   | .19   | .62   | .46   |
|                                | 98.79 | 99.07 | 96.02 | 96.91 | 97.51 | 99.37 | 97.55 | 99.27 | 98.54 |

|    |      |      |      |      |      |      |      |      |      |
|----|------|------|------|------|------|------|------|------|------|
| Si | 6.27 | 6.11 | 7.85 | 6.57 | 7.43 | 7.38 | 6.64 | 6.37 | 6.12 |
| Al | 1.73 | 1.89 | .14  | 1.43 | .57  | .62  | 1.36 | 1.63 | 1.88 |
| Al | 1.10 | 1.24 | .00  | .81  | .40  | .42  | .73  | .86  | .98  |
| Ti | .04  | .04  | .00  | .05  | .02  | .01  | .05  | .04  | .04  |
| Fe | 2.20 | 2.21 | .98  | 1.49 | 1.20 | 1.21 | 1.43 | 2.94 | 2.77 |
| Mn | .05  | .06  | .02  | .03  | .03  | .03  | .04  | .04  | .04  |
| Mg | 1.93 | 1.71 | 4.12 | 2.80 | 3.45 | 3.54 | 2.92 | 1.62 | 1.53 |
| Ca | 1.69 | 1.73 | 1.94 | 1.88 | 1.82 | 1.73 | 1.87 | 1.53 | 1.76 |
| Na | .31  | .27  | .03  | .12  | .18  | .25  | .13  | .47  | .24  |
| Na | .14  | .19  | .00  | .23  | .07  | .00  | .24  | .05  | .25  |
| K  | .07  | .08  | .01  | .06  | .04  | .04  | .04  | .12  | .09  |

|   |      |      |      |      |      |      |      |      |      |
|---|------|------|------|------|------|------|------|------|------|
| Y | 5.32 | 5.26 | 5.12 | 5.18 | 5.10 | 5.21 | 5.17 | 5.50 | 5.36 |
| A | .21  | .27  | .01  | .29  | .11  | .04  | .28  | .17  | .34  |

The zonation of amphibole and plagioclase in the Weinbühel and Tauernkogel Amphibolites shows the prograde evolution of the granoblastic fabric with time. In comparison with the broad albite cores of the plagioclase the small actinolitic cores of the amphibole

suggest that the change in amphibole composition from actinolite to hornblende occurred before the oligoclase isograd was reached. This speaks in favour of a medium-P character for metamorphism (MIYASHIRO, 1973). A medium-P character is also compatible with



the amphibole compositions as shown in Figs. 3 and 4 (for microprobe analyses, see Table 2). Fig. 3 shows the prograde evolution from actinolite (cores and patches of large crystals) to magnesio-hornblende (rims of large crystals and whole small crystals) for the garnet-free Weinbühel and Tauernkogel Amphibolites. A higher metamorphic grade is attested by the increasing Al, Ti, Na, K, and Fe/Mg values. The amphibole composition of the Basis Amphibolite is magnesio-hornblende to tschermakitic hornblende, and reflects the slightly higher metamorphic grade attained in this body.

The temperature increase is indicated by the decreasing Si and the increasing Ti and A-site values. The magnesio- and tschermakitic hornblendes display  $Al^{VI}$  values close to the 5 kb limit of RAASE (1974). Amphiboles plotting above the broken line in the Si- $Al^{VI}$  diagram (Fig. 3) should indicate pressures of more than about 5 kb. Although according to HIETANEN (1974) a pressure estimate from the  $Al^{VI}$  values is very problematic, 5 kb or slightly more at the thermal peak may be a realistic estimate. After HIETANEN (1974) the increasing (Na+K) (A)/ $Al^{VI}$  values (Fig. 3) attest to a decrease in the P/T ratio during metamorphic evolution. Such an interpretation is not confirmed by the diagrams of Fig. 4b and d where the evolution is within the same P-facies series. On the other hand, the Na(M) values, which are about constant in the non-actinolitic hornblendes of the garnet-free amphibolites indicate constant pressure and therefore support the interpretation of a decreasing P/T ratio with time (Figs. 3 and 4a,c) (BROWN, 1977; LAIRD & ALBEE, 1981).

The garnet amphibolites of the Weinbühel and Tauernkogel Complexes have chemical compositions which are markedly richer in iron than those of the other amphibolites. The higher Fe content of the amphiboles (Fig. 3) is due to the rock composition. Ac-

cording to LAIRD & ALBEE (1981) amphiboles from garnetiferous rocks metamorphosed at medium pressures are richer in alumina as those from garnet-free rocks. Therefore the lower Si and higher  $Al^{VI}$  values of the amphiboles from the garnet amphibolites in the diagram of Fig. 3 are also explained by the bulk rock chemistry. Higher pressures and lower temperatures in comparison with the garnet-free rocks are apparently indicated by the diagrams on the right hand side of Fig. 3 and in Fig. 4a, c, d (the diagram Fig. 4b should not be used for garnetiferous rocks because Si and Al are used – see above). In the diagrams of Fig. 4 increasing pressure is in general indicated by the parameter on the abscissa.

P,T calculation based on the ionic activities of the tremolite, glaucophane, edenite, and tschermakite components of amphiboles after the method of HOLLAND & RICHARDSON (1979) show the prograde evolution of the zoned amphiboles from the garnet-free Weinbühel and Tauernkogel Amphibolites. Without being successful in quantifying pressure and temperature, simultaneous increase of both parameters is nevertheless shown by the increasing equilibrium constant K (edenite, tschermakite) and K (glaucophane, tschermakite) from the cores to the rims of the crystals. For the amphiboles from the garnet amphibolites similar K (gl, ts) values for the temperature, but slightly higher K (ed, ts) values for the pressure are obtained. Garnet-hornblende geothermometry after GRAHAM & POWELL (1984) yielded temperatures of 480–490°C for a sample high up in the sequence of the Tauernkogel Complex, and maximum temperatures of 530–550°C for a sample from the Weinbühel Amphibolite. The garnets are almandine-rich and do not contain a major pyrope component (Table 3, Fig. 5). The temperature obtained for the Tauernkogel Amphibolites is about 20°C too low because the An<sub>17</sub> + hornblende isograd has been surpassed, although

Table 3: Microprobe analyses of garnet from the Weinbühel ( $\Delta$ ) and Tauernkogel ( $\circ$ ) Garnet Amphibolites.

Cation concentrations calculated on the basis of 24 oxygens. Symbols as in Fig. 5. C = cores, R = rims of zoned crystals. Shown are also percentages of the spessartine, almandine, grossularite and pyrope contents. See diagrams in Fig. 5.

| Sample                         | $\Delta$ 3 | $\Delta$ 3R | $\circ$ 6 | $\circ$ 6 | $\circ$ 6 | $\circ$ 6 | $\circ$ 6 | $\circ$ 6 | $\circ$ 6C | $\circ$ 6R |
|--------------------------------|------------|-------------|-----------|-----------|-----------|-----------|-----------|-----------|------------|------------|
| SiO <sub>2</sub> %             | 37.90      | 37.94       | 36.78     | 36.95     | 36.76     | 36.57     | 36.32     | 36.56     | 36.90      | 37.01      |
| TiO <sub>2</sub>               | .13        | .14         | .30       | .23       | .00       | .31       | .48       | .68       | .05        | .00        |
| Al <sub>2</sub> O <sub>3</sub> | 21.91      | 22.35       | 20.89     | 20.77     | 21.07     | 20.88     | 20.30     | 20.89     | 21.14      | 21.19      |
| FeO                            | 30.08      | 28.74       | 28.59     | 29.26     | 31.86     | 29.14     | 26.13     | 29.19     | 28.59      | 30.83      |
| MgO                            | 1.16       | 1.21        | .37       | .36       | .96       | .59       | .81       | .74       | 1.23       | .79        |
| MnO                            | 1.39       | 2.49        | 2.00      | 2.10      | .53       | 1.87      | 4.71      | 1.76      | 1.94       | 1.12       |
| CaO                            | 11.48      | 11.74       | 10.08     | 9.80      | 8.15      | 9.54      | 9.46      | 9.14      | 9.11       | 8.63       |
|                                | 104.05     | 104.61      | 99.01     | 99.47     | 99.32     | 98.87     | 98.30     | 98.96     | 98.96      | 99.57      |
| Si                             | 5.87       | 5.83        | 5.97      | 5.98      | 5.96      | 5.95      | 5.95      | 5.93      | 5.97       | 5.98       |
| Al                             | .13        | .17         | .03       | .02       | .04       | .05       | .05       | .07       | .03        | .02        |
| Al                             | 3.87       | 3.88        | 3.96      | 3.94      | 3.99      | 3.95      | 3.88      | 3.93      | 4.00       | 4.01       |
| Ti                             | .01        | .02         | .04       | .03       | .00       | .04       | .06       | .08       | .01        | .00        |
| Fe                             | 3.89       | 3.69        | 3.88      | 3.96      | 4.32      | 3.96      | 3.58      | 3.96      | 3.87       | 4.16       |
| Mn                             | .18        | .32         | .28       | .29       | .07       | .26       | .65       | .24       | .27        | .15        |
| Mg                             | .27        | .28         | .09       | .09       | .23       | .14       | .20       | .18       | .30        | .19        |
| Ca                             | 1.90       | 1.93        | 1.75      | 1.70      | 1.42      | 1.66      | 1.66      | 1.59      | 1.58       | 1.49       |
| spe                            | 3          | 5           | 5         | 5         | 1         | 4         | 11        | 4         | 5          | 3          |
| alm                            | 62         | 60          | 65        | 66        | 72        | 66        | 59        | 66        | 64         | 69         |
| gro                            | 31         | 31          | 29        | 28        | 23        | 28        | 27        | 27        | 26         | 25         |
| pyr                            | 4          | 4           | 1         | 1         | 4         | 2         | 3         | 3         | 5          | 3          |



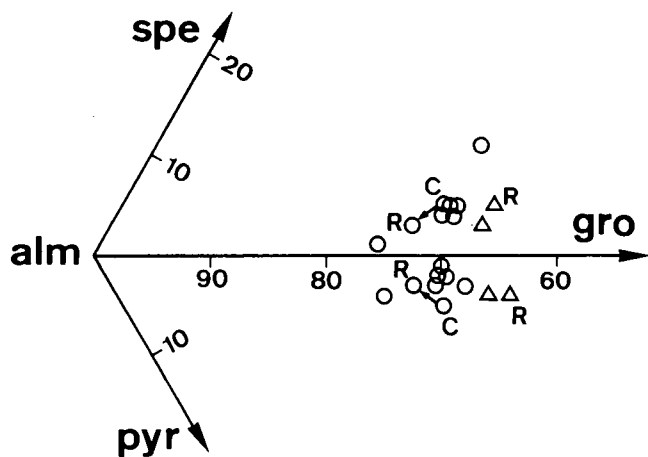


Fig. 5: Diagram showing compositional variation of garnets from garnet amphibolite in a spessartine - almandine - grossularite - pyrope double triangle.  $\Delta$  = Weinbühel Amphibolite;  $\circ$  = Tauernkogel Amphibolite. C, R indicate cores and rims of crystals.

the oligoclase rims are very narrow near the peak of the Tauernkogel. Temperatures of more than 500°C (at about 5 kb) are required (WINKLER, 1979). The temperatures of 530–550°C for the Weinbühel Amphibolite are realistic, for temperatures of slightly more than 550°C may have been attained near the base of the Basis Amphibolite east of Felbertauern (see above). The temperature increase from the Tauernkogel to the Basis Amphibolites is compatible with a thermal gradient typical of medium-P type metamorphic terrains (20–25°C/km) taking into consideration a flat-lying sequence at the peak of Alpine metamorphism and later tilting to the west due to the updoming of the Granatspitz Zentralgneis cupola.

The An<sub>17</sub> + hornblende isograd has also been exceeded in the Felbertal mine and the Stubachtal Complex. In the Stubachtal Complex re-equilibrated polysynthetically twinned plagioclase is preserved. The amphibolites contain garnet in places.

Relict rutile, partly replaced by sphene, is present in several samples. Frequently it forms inclusions in hornblende. It is either a relic of the igneous stage or of an older, possibly high-pressure metamorphic event. Lawsonite pseudomorphs within the Basis Amphibolite Complex in the Felbertauern road tunnel were reported by FRISCH (1984) and support the idea of an older high-pressure event. The prograde P,T evolution of the granuloblastic fabric of the amphibolites, however, suggests that this older event was separated in time from Alpine regional metamorphism, whose peak was reached around the Eocene/Oligocene boundary.

Relict hornblende from the Zwölferzug Amphibolite, which is an equivalent of the Basis amphibolite farther north in the Felber Tal, was dated radiometrically by PESTAL (1983). He obtained K/Ar ages around 320 Ma. Alpine metamorphism remained there below the hornblende-oligoclase isograd.

#### 4. Geochemistry

From the field relations and the geochemistry of the rocks it is deduced that the different basic complexes investigated in this study belong to two genetically dif-

ferent geotectonic sequences which formed a primary succession. The chemical analyses are listed in Table 4. Variation diagrams and the AFM diagram are shown in Figs. 6 and 7 respectively; MORB (mid ocean ridge basalt) normalised diagrams after PEARCE et al. (1981) and PEARCE (1982) for rocks with a silica content of basalts or basaltic andesites are presented in Fig. 8. For comparison, basaltic suites from different tectonic settings are shown in Fig. 9 (PEARCE, 1982). The TiO<sub>2</sub>-Zr diagram after PEARCE (1979, 1982) (Fig. 10) and the diagrams after MIYASHIRO & SHIDO (1975) using the FeO\*/MgO ratio as a fractionation index (Fig. 11) also allow for more acidic rocks. Basaltic and andesitic rocks are plotted in the Ti-V diagram after SHERVAIS (1982) (Fig. 12). The diagrams after MULLEN (1983) (Fig. 13), PEARCE & CANN (1973) (Fig. 14), and MESCHÉDE (1986) (Fig. 15) are suited for the discrimination of basaltic rocks. In Fig. 13 basaltic andesites are plotted as well. In the following the geochemistry is discussed separately for each investigated complex.

#### 4.1. The Stubachtal Complex

Ultrabasic rocks make up the great part of this classical locality (WEINSCHENK, 1894; BECKE, 1895; CORNELIUS & CLAR, 1939; PETRAKAKIS, 1977), which is part of the Basis Amphibolite sequence. The mafic members exhibit fine-grained texture and are to be classified as metabasalts. In the AFM diagram (Fig. 7) these rocks show a more tholeiitic trend than the basaltic rocks from the other complexes. The tholeiitic character is confirmed by the high FeO\* and low Al<sub>2</sub>O<sub>3</sub> values (Fig. 6). Relatively low CaO and high Na<sub>2</sub>O values suggest some spilitisation (Fig. 6). In the MORB normalised diagram (Fig. 8) the Stubachtal meta-basalts follow a rather flat trend close to unity for the elements Nb, P, Zr, Ti, and Y. Enrichment in elements with low ionic potential, in particular K, Rb, and Ba, relative to MORB is a characteristic of subduction-related magmas. The mobility of these elements during metamorphism, however, places the reliability of this feature in doubt. On the other hand the low abundance of the compatible element Cr is also in agreement with an arc component. The Cr is removed by fractional crystallisation (e. g. PEARCE, 1982). While island arc basalts also show depletion of other elements with high ionic potential, the MORB normalised pattern of the Stubachtal metabasalts very closely resembles that of the Geotimes unit in the Oman ophiolite complex (Fig. 9a, PEARCE et al., 1981). A slight negative anomaly for Ti is exhibited in both cases and is considered to be due to the fractionation of a titanium-bearing phase (titano-magnetite) in a melt with elevated oxygen fugacity. The Geotimes unit is interpreted by PEARCE et al. (1981) as backarc oceanic crust, an interpretation which can also be meaningfully applied to the Basis Amphibolite Complex, to which the Stubachtal Complex belongs.

In the TiO<sub>2</sub>-Zr diagram (Fig. 10) the Stubachtal metabasalts again occupy the same field as the Geotimes rocks (PEARCE et al., 1981). The tholeiitic or intermediate tholeiitic to calc-alkaline character of the Stubachtal rocks is shown in the diagram in Fig. 11. In the Ti-V diagram (Fig. 12) they plot into the large overlap area of the MORB and back-arc basalt fields. A MORB character is also displayed in the diagrams in Figures 14 and 15, which use relatively immobile ele-

Table 4: Chemical (XRF) analyses of ultramafic rocks, amphibolites and acid volcano-detrital rocks from the Stubachtal ultramafic/mafic body, the Felbertal scheelite mine, the Basis Amphibolite east of Felbertauern, the Weinbühel and the Tauernkogel Amphibolites.

Symbols as in Fig. 6; nd = not determined. Dashes indicate values below the detection limit, i.e. CaO = 0.20, Na<sub>2</sub>O = 0.12, K<sub>2</sub>O = 0.10, P<sub>2</sub>O<sub>5</sub> = 0.01 %; Ba = 54, Cr = 49, Nb = 62, Rb = 4, Sr = 5, V = 13, Y = 15, Zr = 34 ppm. See diagrams in Figs. 6–8 and 10–15.

| Sample                         | ◆1923 | ◆1924 | ◆1935 | ◆1916 | ◆1918 | ◆1925 | ●1934 | ●1930 | ●1931 | ●1926 | ●1932 | ●1929 | ■2328 |
|--------------------------------|-------|-------|-------|-------|-------|-------|-------|-------|-------|-------|-------|-------|-------|
| SiO <sub>2</sub> %             | 39.41 | 39.52 | 39.34 | 39.94 | 39.77 | 48.65 | 48.72 | 49.83 | 50.03 | 50.06 | 51.74 | 54.76 | 46.06 |
| TiO <sub>2</sub>               | .04   | .04   | --    | --    | --    | .07   | 1.52  | 1.22  | 1.47  | 1.69  | 1.30  | 1.31  | 1.19  |
| Al <sub>2</sub> O <sub>3</sub> | 1.04  | 1.12  | .58   | 1.16  | .92   | 1.50  | 14.15 | 14.56 | 14.07 | 13.97 | 15.90 | 14.23 | 15.84 |
| Fe <sub>2</sub> O <sub>3</sub> | 1.73  | 1.39  | 3.69  | 4.15  | 5.25  | .79   | 1.38  | 1.14  | 1.84  | 1.25  | .99   | .53   | 2.09  |
| FeO                            | 7.82  | 8.12  | 4.85  | 4.25  | 4.33  | 4.28  | 11.27 | 10.25 | 10.77 | 11.50 | 10.47 | 10.95 | 10.27 |
| MnO                            | .16   | .15   | .14   | .19   | .19   | .11   | .25   | .23   | .20   | .24   | .24   | .26   | .23   |
| MgO                            | 44.76 | 44.31 | 40.03 | 39.97 | 39.76 | 23.78 | 6.64  | 6.40  | 6.49  | 5.43  | 4.75  | 4.14  | 8.39  |
| CaO                            | 1.72  | 1.61  | --    | 2.57  | 3.02  | 16.52 | 8.32  | 9.13  | 6.53  | 7.72  | 6.26  | 5.56  | 10.41 |
| Na <sub>2</sub> O              | .17   | .14   | .12   | .15   | --    | .13   | 3.82  | 4.10  | 4.31  | 4.58  | 5.64  | 4.98  | 2.53  |
| K <sub>2</sub> O               | --    | --    | --    | --    | --    | --    | .19   | .18   | .61   | .29   | .18   | .18   | .57   |
| P <sub>2</sub> O <sub>5</sub>  | --    | --    | --    | --    | --    | --    | .13   | .10   | .16   | .20   | .10   | .22   | .17   |
| LOI                            | 2.46  | 2.56  | 9.66  | 6.50  | 5.92  | 2.55  | 2.12  | 2.07  | 2.36  | 2.12  | 1.89  | 1.88  | 1.88  |
|                                | 99.31 | 98.36 | 98.41 | 98.88 | 99.16 | 98.38 | 98.51 | 99.21 | 98.84 | 99.10 | 99.46 | 98.93 | 99.64 |
| Ba ppm                         | --    | --    | --    | --    | --    | --    | 91    | 114   | 211   | 157   | 74    | 73    | 170   |
| Cr                             | 4794  | 4195  | 6058  | 3906  | 4511  | 3385  | 78    | 164   | 97    | 64    | --    | 46    | 284   |
| Nb                             | --    | --    | --    | --    | --    | --    | --    | --    | --    | 7     | --    | --    | --    |
| Ni                             | 2277  | 2338  | 2773  | 2178  | 2076  | 772   | 30    | 47    | 30    | --    | 16    | --    | 98    |
| Rb                             | --    | --    | --    | --    | 8     | --    | 7     | --    | 26    | 9     | --    | --    | 19    |
| Sr                             | 59    | 28    | --    | --    | 15    | 25    | 104   | 265   | 92    | 127   | 182   | 123   | 308   |
| V                              | 40    | 40    | 41    | 52    | 56    | 169   | 303   | 308   | 315   | 354   | 248   | 230   | 282   |
| Y                              | --    | --    | --    | --    | --    | --    | 36    | 23    | 33    | 33    | 39    | 40    | 25    |
| Zn                             | 53    | 52    | 122   | 52    | 46    | 19    | 168   | 145   | 153   | 124   | 148   | 193   | 133   |
| Zr                             | --    | --    | --    | --    | --    | --    | 102   | 84    | 91    | 107   | 139   | 121   | 83    |

| Sample                         | ■2331 | ■2338 | ■2335  | ■2330 | ■ B2  | ■2337  | ■2336 | ■ B3  | ■2333 | +2384 | +2377 | +2378 | +2382 |
|--------------------------------|-------|-------|--------|-------|-------|--------|-------|-------|-------|-------|-------|-------|-------|
| SiO <sub>2</sub> %             | 48.94 | 49.28 | 51.01  | 51.53 | 53.35 | 53.37  | 53.57 | 54.03 | 54.74 | 49.48 | 47.90 | 50.15 | 50.18 |
| TiO <sub>2</sub>               | 1.42  | 1.22  | 1.56   | 1.32  | 1.08  | 1.65   | 1.70  | 1.07  | .95   | 1.04  | 1.33  | 1.28  | .89   |
| Al <sub>2</sub> O <sub>3</sub> | 18.47 | 18.67 | 14.79  | 17.95 | 18.14 | 15.32  | 17.86 | 16.94 | 15.54 | 16.24 | 14.87 | 14.74 | 17.04 |
| Fe <sub>2</sub> O <sub>3</sub> | 2.11  | 2.26  | 3.26   | 2.14  | 2.49  | 3.45   | 2.54  | 1.82  | 1.67  | 2.02  | 2.79  | 1.28  | 1.76  |
| FeO                            | 7.11  | 6.39  | 6.60   | 6.45  | 5.17  | 7.02   | 4.45  | 6.18  | 6.53  | 6.89  | 7.78  | 7.79  | 7.02  |
| MnO                            | .15   | .13   | .18    | .13   | .13   | .19    | .11   | .10   | .17   | .21   | .24   | .17   | .16   |
| MgO                            | 5.74  | 6.14  | 7.09   | 5.12  | 4.28  | 5.57   | 4.75  | 4.47  | 5.54  | 6.45  | 8.44  | 7.59  | 5.13  |
| CaO                            | 9.24  | 9.31  | 9.68   | 8.38  | 7.54  | 8.36   | 9.01  | 9.01  | 7.38  | 11.77 | 11.19 | 11.57 | 9.86  |
| Na <sub>2</sub> O              | 3.86  | 3.68  | 3.30   | 4.46  | 4.14  | 2.93   | 3.96  | 3.50  | 4.61  | 2.91  | 2.28  | 2.81  | 3.40  |
| K <sub>2</sub> O               | .53   | .33   | .55    | .50   | .78   | .79    | .45   | .24   | .86   | .70   | .88   | .37   | .58   |
| P <sub>2</sub> O <sub>5</sub>  | .35   | .31   | .15    | .33   | .14   | .18    | .09   | .10   | .11   | .08   | .12   | .12   | .10   |
| LOI                            | 1.66  | 1.95  | 1.84   | 1.29  | 1.24  | 1.67   | 1.34  | 1.45  | 1.45  | 1.66  | 1.81  | 1.87  | 2.18  |
|                                | 99.58 | 99.67 | 100.01 | 99.74 | 98.48 | 100.50 | 99.83 | 98.91 | 99.55 | 99.45 | 99.63 | 99.74 | 98.30 |
| Ba ppm                         | 198   | 180   | 186    | 278   | nd    | 349    | 195   | nd    | 396   | 279   | 348   | 133   | 460   |
| Cr                             | 143   | 137   | 247    | 139   | 33    | 122    | --    | 43    | 132   | 358   | 255   | 260   | 257   |
| Nb                             | 7     | 9     | --     | 7     | nd    | --     | 8     | nd    | --    | --    | --    | --    | --    |
| Ni                             | --    | 67    | --     | --    | 29    | --     | --    | 22    | --    | 110   | 66    | 70    | 81    |
| Rb                             | 12    | --    | 15     | 17    | 14    | 17     | 9     | 4     | 55    | 76    | 124   | 27    | 89    |
| Sr                             | 745   | 920   | 274    | 602   | 699   | 281    | 429   | 388   | 294   | 202   | 169   | 192   | 311   |
| V                              | 202   | 198   | 269    | 190   | nd    | 271    | 206   | nd    | 222   | 278   | 336   | 300   | 238   |
| Y                              | --    | --    | 21     | --    | 18    | 24     | --    | 21    | 23    | 24    | 36    | 23    | 25    |
| Zn                             | 112   | 88    | 93     | 103   | nd    | 94     | 58    | nd    | 157   | 106   | 116   | 82    | 82    |
| Zr                             | 158   | 161   | 117    | 152   | 149   | 137    | 90    | 108   | 59    | 59    | 76    | 69    | 66    |

| Sample                         | +2380 | +2381 | +2379  | Δ2347  | Δ2346 | Δ2374  | Δ H4  | Δ H1  | Δ2373  | Δ2348  | Δ2349  | Δ2351  | Δ2350 |
|--------------------------------|-------|-------|--------|--------|-------|--------|-------|-------|--------|--------|--------|--------|-------|
| SiO <sub>2</sub> %             | 50.81 | 51.34 | 51.94  | 51.28  | 51.95 | 54.04  | 56.53 | 57.24 | 54.04  | 55.11  | 55.45  | 65.63  | 67.30 |
| TiO <sub>2</sub>               | 1.19  | 1.06  | .95    | .45    | .52   | .57    | .51   | .47   | 1.33   | 1.14   | 1.16   | .53    | .50   |
| Al <sub>2</sub> O <sub>3</sub> | 14.43 | 15.76 | 14.36  | 16.59  | 16.97 | 15.39  | 16.53 | 16.68 | 15.19  | 14.77  | 14.84  | 15.58  | 14.70 |
| Fe <sub>2</sub> O <sub>3</sub> | 1.41  | 2.22  | 1.28   | 3.50   | 2.39  | 2.48   | 2.01  | 1.51  | 2.54   | 3.50   | 3.54   | 2.11   | 1.96  |
| FeO                            | 8.67  | 7.08  | 7.33   | 6.33   | 6.49  | 7.37   | 6.32  | 6.32  | 11.04  | 9.30   | 9.25   | 5.10   | 4.64  |
| MnO                            | .20   | .17   | .16    | .17    | .15   | .20    | .16   | .15   | .24    | .24    | .23    | .14    | .13   |
| MgO                            | 7.43  | 6.10  | 8.32   | 6.85   | 6.19  | 6.46   | 3.82  | 4.15  | 3.68   | 3.60   | 3.59   | 1.03   | .97   |
| CaO                            | 9.45  | 8.88  | 10.54  | 10.43  | 9.39  | 7.87   | 6.85  | 7.29  | 7.41   | 7.71   | 7.74   | 4.79   | 4.63  |
| Na <sub>2</sub> O              | 3.42  | 3.55  | 2.95   | 1.78   | 3.81  | 3.86   | 3.93  | 2.92  | 2.86   | 2.73   | 2.82   | 3.86   | 3.64  |
| K <sub>2</sub> O               | .49   | .97   | .42    | .31    | .40   | .28    | .22   | .49   | .22    | .28    | .40    | .49    | .52   |
| P <sub>2</sub> O <sub>5</sub>  | .12   | .09   | .07    | .04    | .05   | .06    | .05   | .06   | .28    | .10    | .11    | .12    | .12   |
| LOI                            | 1.80  | 1.96  | 1.74   | 2.58   | 1.64  | 1.65   | 1.35  | 1.51  | 1.41   | 1.53   | 1.58   | .98    | .86   |
|                                | 99.42 | 99.18 | 100.06 | 100.31 | 99.95 | 100.23 | 98.28 | 98.79 | 100.24 | 100.01 | 100.71 | 100.36 | 99.97 |
| Ba ppm                         | 129   | 370   | 102    | 99     | 152   | 74     | nd    | nd    | 95     | 92     | 195    | 245    | 286   |
| Cr                             | 226   | 345   | 345    | 66     | 115   | --     | 15    | 12    | --     | --     | --     | --     | --    |
| Nb                             | --    | --    | --     | --     | --    | --     | nd    | nd    | --     | --     | --     | --     | --    |
| Ni                             | 67    | 131   | 104    | --     | --    | --     | 11    | 8     | --     | --     | --     | --     | --    |
| Rb                             | 48    | 118   | 50     | 13     | 11    | --     | 3     | 13    | --     | --     | 9      | 17     | 16    |
| Sr                             | 85    | 178   | 119    | 197    | 221   | 326    | 251   | 272   | 138    | 181    | 158    | 181    | 203   |
| V                              | 288   | 291   | 255    | 245    | 257   | 246    | nd    | nd    | 199    | 371    | 358    | 48     | 47    |
| Y                              | 24    | 28    | 19     | --     | --    | --     | 26    | 14    | --     | --     | --     | --     | --    |
| Zn                             | 100   | 103   | 87     | 103    | 152   | 91     | nd    | nd    | 108    | 127    | 116    | 101    | 103   |
| Zr                             | 57    | 56    | 54     | --     | 39    | 63     | 73    | 67    | 45     | 53     | 51     | 88     | 121   |

Table 4 (continued).

| Sample                         | Δ2353 | Δ2341 | Δ2320 | Δ H2  | Δ2321 | Δ2342  | Δ2322 | Δ2323 | Δ2324 | Δ2325 | ○ R3  | ○2360  | ○2362 |
|--------------------------------|-------|-------|-------|-------|-------|--------|-------|-------|-------|-------|-------|--------|-------|
| SiO <sub>2</sub> %             | 68.53 | 52.48 | 56.21 | 56.60 | 57.98 | 58.19  | 60.28 | 65.63 | 66.35 | 69.58 | 48.38 | 54.62  | 55.88 |
| TiO <sub>2</sub>               | .46   | .82   | .77   | .76   | .83   | .88    | .81   | .65   | .53   | .37   | .60   | .58    | .64   |
| Al <sub>2</sub> O <sub>3</sub> | 14.29 | 18.41 | 17.27 | 15.05 | 16.54 | 16.40  | 16.38 | 14.23 | 15.86 | 15.21 | 17.46 | 13.50  | 14.00 |
| Fe <sub>2</sub> O <sub>3</sub> | 1.68  | 1.93  | 2.85  | 2.56  | 2.52  | 1.74   | 2.37  | 2.28  | 1.72  | 1.35  | 2.87  | 1.63   | 1.46  |
| FeO                            | 4.36  | 6.06  | 4.16  | 4.78  | 4.41  | 4.87   | 3.89  | 3.52  | 2.24  | 1.57  | 4.89  | 5.37   | 5.29  |
| MnO                            | .12   | .18   | .12   | .12   | .12   | .11    | .10   | .09   | .07   | .05   | .17   | .14    | .12   |
| MgO                            | .88   | 5.30  | 4.83  | 5.38  | 4.43  | 4.83   | 3.19  | 2.98  | 2.22  | 1.51  | 7.70  | 9.80   | 8.64  |
| CaO                            | 4.29  | 6.26  | 6.23  | 7.69  | 5.69  | 6.30   | 5.61  | 3.35  | 3.32  | 3.41  | 11.46 | 8.00   | 7.93  |
| Na <sub>2</sub> O              | 3.80  | 5.41  | 4.78  | 4.05  | 5.38  | 4.17   | 4.83  | 4.91  | 5.62  | 4.93  | 2.54  | 2.86   | 2.85  |
| K <sub>2</sub> O               | .47   | .38   | .22   | .27   | .14   | .37    | .14   | .16   | .23   | .33   | .63   | 1.24   | 1.06  |
| P <sub>2</sub> O <sub>5</sub>  | .12   | .35   | .29   | .18   | .25   | .34    | .23   | .18   | .24   | .15   | .07   | .12    | .13   |
| LOI                            | .85   | 2.06  | 2.08  | 1.43  | 1.66  | 1.92   | 1.67  | 1.71  | 1.52  | 1.28  | 2.63  | 2.16   | 1.91  |
|                                | 99.85 | 99.64 | 99.81 | 98.87 | 99.95 | 100.12 | 99.92 | 99.69 | 99.92 | 99.74 | 99.40 | 100.02 | 99.91 |
| Ba ppm                         | 224   | 167   | 99    | nd    | 65    | 204    | 80    | --    | 121   | 233   | nd    | 369    | 247   |
| Cr                             | --    | 88    | 58    | 106   | 82    | 59     | 58    | --    | 59    | --    | 144   | 539    | 447   |
| Nb                             | 7     | 19    | 15    | nd    | 13    | 15     | 13    | 14    | 13    | 15    | nd    | --     | --    |
| Ni                             | --    | --    | --    | 16    | --    | --     | --    | --    | --    | --    | 44    | 144    | 117   |
| Rb                             | 16    | 13    | --    | 3     | --    | 11     | --    | 9     | 9     | 17    | 19    | 44     | 34    |
| Sr                             | 189   | 491   | 912   | 931   | 548   | 769    | 899   | 460   | 811   | 817   | 468   | 316    | 436   |
| V                              | 34    | 188   | 191   | nd    | 184   | 183    | 159   | 115   | 89    | 63    | nd    | 157    | 164   |
| Y                              | --    | --    | --    | 20    | --    | --     | --    | --    | --    | --    | 16    | --     | --    |
| Zn                             | 95    | 110   | 53    | nd    | 57    | 71     | 40    | 35    | 32    | 21    | nd    | 67     | 62    |
| Zr                             | 104   | 312   | 223   | 203   | 194   | 225    | 223   | 232   | 220   | 193   | 75    | 94     | 108   |

| Sample                         | ○2367 | ○ R4  | ○2365 | ○ R8  | ○2366 | ○ R2  | ○2358  | ◇ R10 | ◇2343 | ◇2344 | ◇ H5  | ◇2372 | ◇2345 |
|--------------------------------|-------|-------|-------|-------|-------|-------|--------|-------|-------|-------|-------|-------|-------|
| SiO <sub>2</sub> %             | 46.94 | 47.28 | 48.35 | 48.57 | 48.72 | 55.35 | 55.36  | 74.63 | 75.56 | 75.83 | 75.85 | 76.08 | 76.40 |
| TiO <sub>2</sub>               | 1.08  | 1.10  | 1.03  | 1.00  | 1.08  | .57   | 1.18   | .18   | .15   | .14   | .15   | .21   | .15   |
| Al <sub>2</sub> O <sub>3</sub> | 19.51 | 20.12 | 19.33 | 19.67 | 18.97 | 15.86 | 16.24  | 13.51 | 13.09 | 13.45 | 11.86 | 11.97 | 13.07 |
| Fe <sub>2</sub> O <sub>3</sub> | 3.88  | 4.02  | 3.07  | 2.92  | 3.70  | 2.13  | 2.38   | .74   | 1.36  | .82   | .63   | 2.08  | 1.38  |
| FeO                            | 6.27  | 5.03  | 6.55  | 6.00  | 5.89  | 4.47  | 4.50   | .72   | .85   | 1.14  | 2.28  | .98   | .59   |
| MnO                            | .19   | .13   | .19   | .19   | .16   | .15   | .16    | .04   | .02   | .02   | .06   | .05   | .01   |
| MgO                            | 4.81  | 4.11  | 4.49  | 4.34  | 4.82  | 5.91  | 5.07   | .37   | .37   | .54   | .72   | .21   | .43   |
| CaO                            | 9.15  | 9.29  | 8.92  | 7.54  | 8.63  | 9.25  | 7.30   | 1.70  | 1.64  | --    | 2.94  | 1.86  | --    |
| Na <sub>2</sub> O              | 3.16  | 3.15  | 3.53  | 3.31  | 3.38  | 2.90  | 5.59   | 3.83  | 3.98  | 3.42  | 3.60  | 4.02  | 3.64  |
| K <sub>2</sub> O               | 2.25  | 1.60  | 1.75  | 2.80  | 2.12  | 1.21  | .57    | .90   | 1.56  | 1.88  | .27   | 1.35  | 2.10  |
| P <sub>2</sub> O <sub>5</sub>  | .54   | .40   | .54   | .20   | .52   | .13   | .22    | .02   | .04   | .02   | .03   | .04   | .03   |
| LOI                            | 2.06  | 2.13  | 2.02  | 1.85  | 1.94  | 1.67  | 1.61   | .76   | 1.08  | 1.46  | .95   | .90   | 1.23  |
|                                | 99.84 | 98.37 | 99.77 | 98.39 | 99.96 | 99.67 | 100.18 | 99.40 | 99.70 | 98.72 | 99.34 | 99.75 | 99.03 |
| Ba ppm                         | 1776  | nd    | 1580  | nd    | 1579  | nd    | 159    | nd    | 522   | 352   | nd    | 504   | 1078  |
| Cr                             | --    | 2     | --    | --    | --    | 111   | 59     | --    | --    | --    | --    | --    | --    |
| Nb                             | 9     | nd    | 9     | nd    | 10    | nd    | --     | nd    | 7     | --    | nd    | 7     | --    |
| Ni                             | --    | 4     | --    | 12    | --    | 55    | --     | 10    | --    | --    | 12    | --    | --    |
| Rb                             | 93    | 47    | 74    | 110   | 98    | 51    | 22     | 99    | 42    | 60    | 7     | 38    | 53    |
| Sr                             | 750   | 727   | 735   | 640   | 609   | 554   | 397    | 301   | 159   | 119   | 454   | 170   | 80    |
| V                              | 221   | nd    | 223   | nd    | 201   | nd    | 208    | nd    | --    | 13    | nd    | --    | --    |
| Y                              | 32    | 37    | 29    | 30    | 33    | 20    | 22     | 16    | 17    | 24    | 12    | 20    | 20    |
| Zn                             | 100   | nd    | 92    | nd    | 92    | nd    | 78     | nd    | 25    | 29    | nd    | 68    | 34    |
| Zr                             | 195   | 194   | 207   | 187   | 234   | 157   | 189    | 150   | 114   | 109   | 241   | 158   | 107   |

ments with high ionic potential. The according fields, however, also allow for arc-related basalts. In the Ti-Mn-P diagram (Fig. 13) the subduction-related component again becomes evident. The passive enrichment of MnO relative to N-type MORB can be explained by fractionation of titanium by crystallisation of a titanium-bearing phase (see above), and a relatively low degree of partial melting, because P is not depleted. Such an interpretation is in agreement with MULLEN (1983) and is able to explain the position of the Stubachtal metabasalts in the diagram.

The geochemical pattern of the Stubachtal basaltic amphibolites best correlates with back-arc oceanic crust. Both the oceanic crust and arc components are discernible. The oceanic crust character is supported by the accompanying ultramafic rocks which contain primary dunites and layered (cumulate) peridotites. The Ni and Cr abundances of the dunites and harzburgites correspond with those of dunites and harzburgites from ophiolitic complexes. The metamorphic paragenesis olivine-antigorite has been described by WEINSCHENK (1894) and CORNELIUS & CLAR (1939).

## 4.2. The Basis Amphibolite East of Felbertauern

From the texture this is a gabbroic body which suffered strong deformation. Changes in the amphibolite/plagioclase ratio are considered to be mainly due to metamorphic differentiation. Irregularities in the element concentrations, especially for the more mobile elements, speak in favour of this interpretation (Fig. 6). The plutonic character of the rock may also be responsible for differences in chemistry. According to the SiO<sub>2</sub> content the metagabbro ranges into the dioritic field (Fig. 6). Figures 6 and 7 display a more calc-alkaline character for the metagabbro in comparison with the Stubachtal metabasalts. This is evidenced by lower FeO\* and higher Al<sub>2</sub>O<sub>3</sub> and K<sub>2</sub>O values (Fig. 6), and a lower FeO\*/MgO ratio (Fig. 7).

In the MORB normalised diagram (Fig. 8) the trend of enrichment of elements with low ionic potential relative to those with high ionic potential is more emphasised. This is interpreted in terms of a stronger subduction-re-

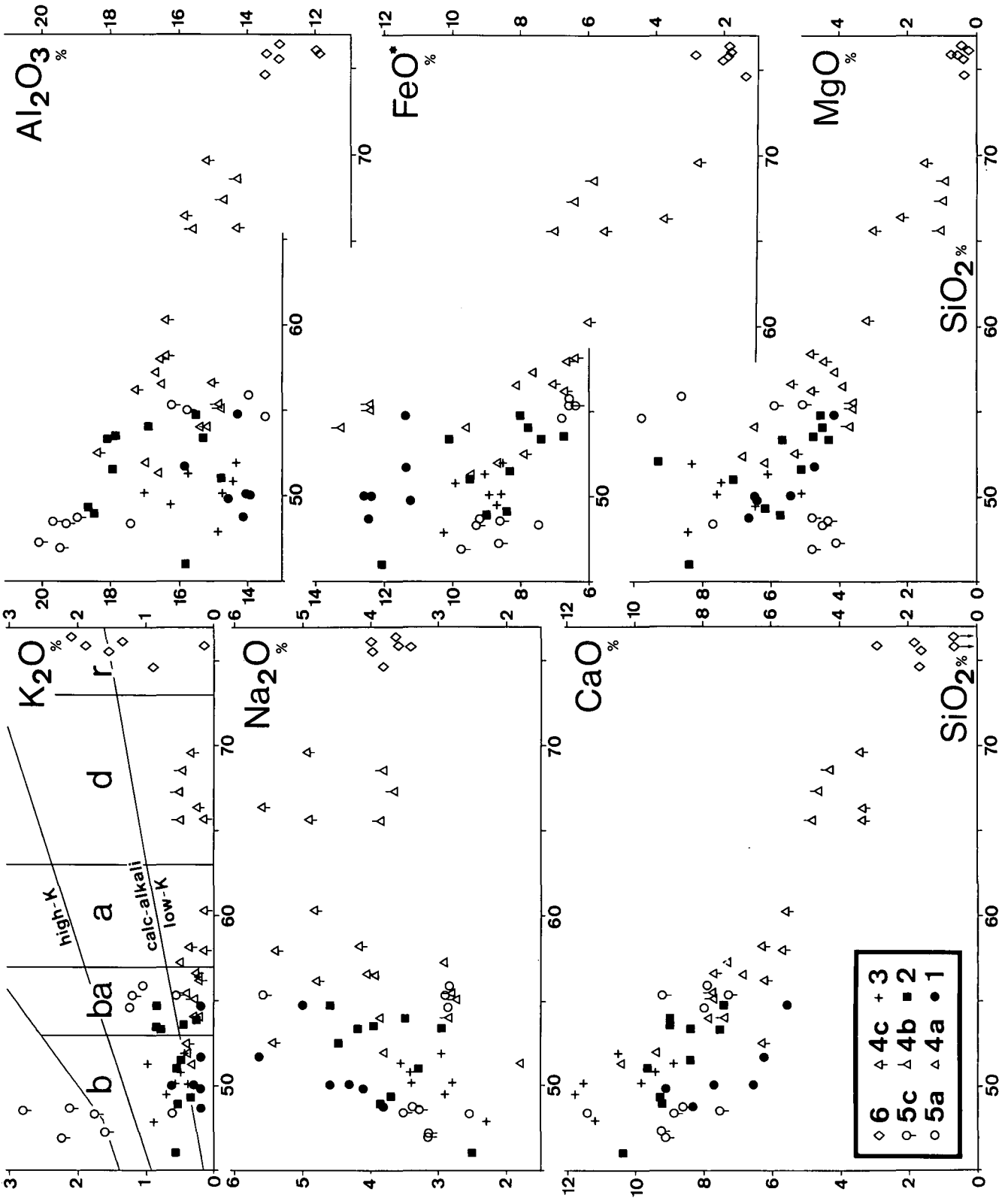


Fig. 6  
Variation diagram of main elements versus silica.  
Upper left shows subdivisions into b = basalt, ba = basaltic andesite; a = andesite; d = dacite; r = rhyolite. Also shown are low-K, medium-K (calc-alkaline) and high-K series after EWART (1982). FeO\* is total iron.  
Symbols: 1 = amphibolites from Subachtal (Basis Amphibolite Complex); 2 = Gabbroic Basis Amphibolite east of Felbertauern; 3 = Felbertal mine amphibolites; 4 = Weinbühel Amphibolites (a = chemically relatively unmodified rocks; b = unmodified tholeiitic rocks; c = rocks enriched in immobile trace elements by deformation = "chemically modified" rocks); 5 = Tauernkogel Amphibolites (a = chemically relatively unmodified rocks; c = rocks enriched in immobile trace elements by deformation = "chemically modified" rocks); 6 = volcano-detritical rocks intercalated with the Weinbühel (5 samples) and the Tauernkogel (1 sample) Amphibolites (note that they may contain a non-volcanic component).

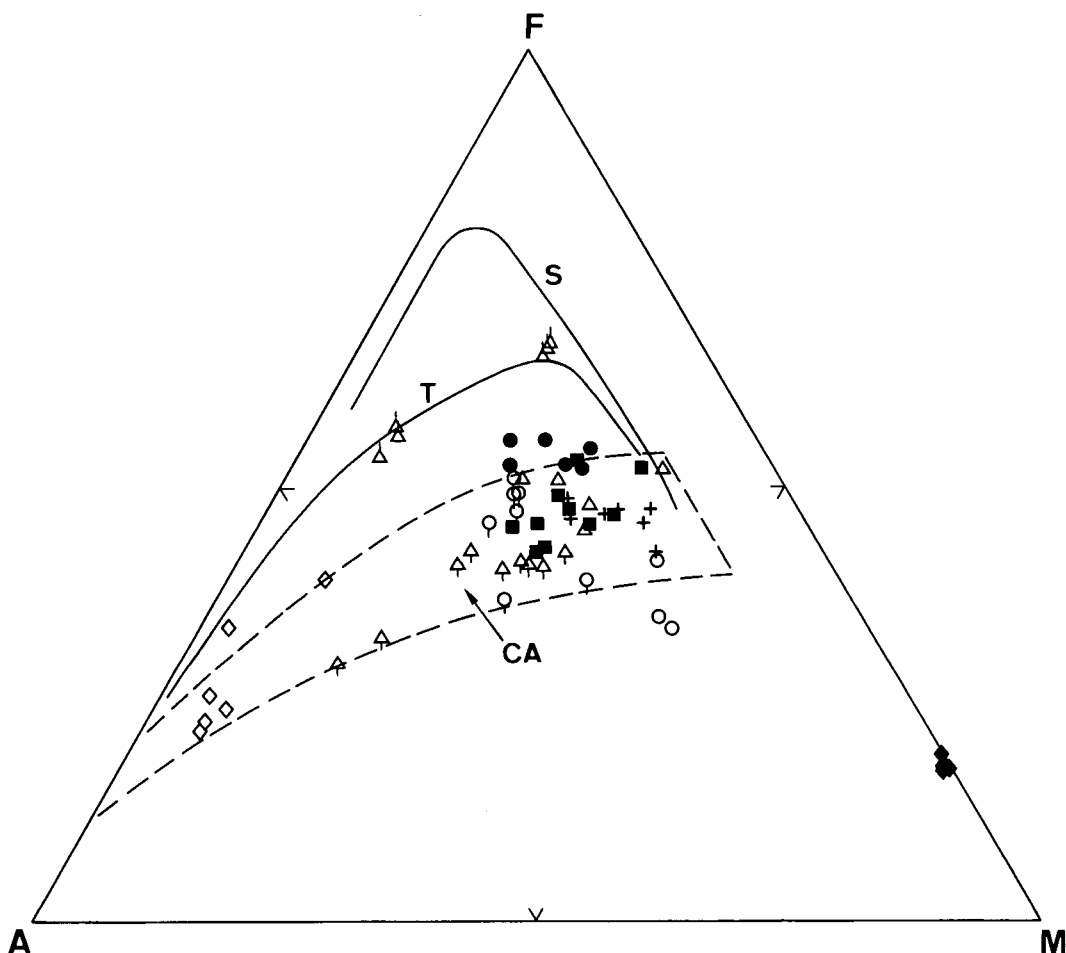


Fig. 7: AFM diagram showing the variations of the amphibolite sequences. Symbols as in Fig. 6.  $\blacklozenge$  near FM line are ultramafic rocks from Stubachtal ultramafic/mafic body. CA = calc-alkaline trend of Cascades; T = tholeiitic trend of Thingmuli, Iceland; S = tholeiitic trend of Skaergard, Greenland (after RINGWOOD, 1975). Note that "chemically unmodified" Weinbühel Amphibolites plot toward the upper half of the calc-alkaline field. Tauernkogel Amphibolites plot differently, which is suggested to be caused by metasomatic influence from the Venediger Zentralgneis.

lated component for the metagabbro compared to the Stubachtal metabasalts. The relatively high abundances of P and Zr could be explained by low amounts of partial melting, but the depletion of Y suggests the opposite. Inhomogeneities in the mantle source may therefore give a better explanation. Another explanation, which is preferred here, is that immobile trace elements were passively enriched during the mylonitisation of the Basis Amphibolite east of Felbertauern. There is a correlation between the intensity of deformation and the abundance of immobile trace elements and modal contents of accessory phases like apatite and sphene in distinct shear zones of the Weinbühel and Tauernkogel Amphibolites (see below). Geochemical work on amphibolites in the Silvretta (Austroalpine Basement Complex) clearly shows that the abundances of Ti, P, and Zr in shear zones have raised to two to five times their original values by the emigration of main elements and passive enrichment of sphene, apatite, and zircon (BRÖCKER, 1985). The increase in Y was only half as that of the other elements in the Silvretta rocks due to its affinity for both immobile mineral phases (mainly apatite) and amphibole which broke down to chlorite or recrystallised completely. Nb was not analysed in the Silvretta samples, and is below the detection limit in most samples of the gabbroic Basis Amphibolite. Some samples, however, show enrichment of Nb relative to

MORB indicating possible concentration of this element during deformation.

The diagram in Fig. 10 shows the agreement of the gabbroic amphibolites with the basaltic ones of Stubachtal, but also a tendency to intermediate source rocks. Fig. 11 shows a more calc-alkaline affinity than the Stubachtal amphibolites. The same tendency is shown by slightly lower average Ti and V values (Fig. 12). The considerably larger scatter in the diagrams of Figs. 13 to 15 may partly be due to the strong deformation but is also compatible with a greater subduction-related component or the intrusive character of the rocks.

The similarity between the metagabbroic amphibolite east of Felbertauern and the metabasaltic amphibolite of the Stubachtal locality is evident, and therefore a back-arc environment is also proposed for those rocks. In the  $TiO_2$ -Zr diagram (Fig. 10) in particular both rock suites plot on the "axis" side of the dividing line drawn for the Oman rocks, where the back-arc suites are located (PEARCE et al., 1981). The metagabbro has a stronger arc component than the Stubachtal rocks, as particularly evidenced by the high  $Al_2O_3$  and low Y contents. The metagabbro may be an intrusion into back-arc oceanic crust in a supra-subduction seamount setting.

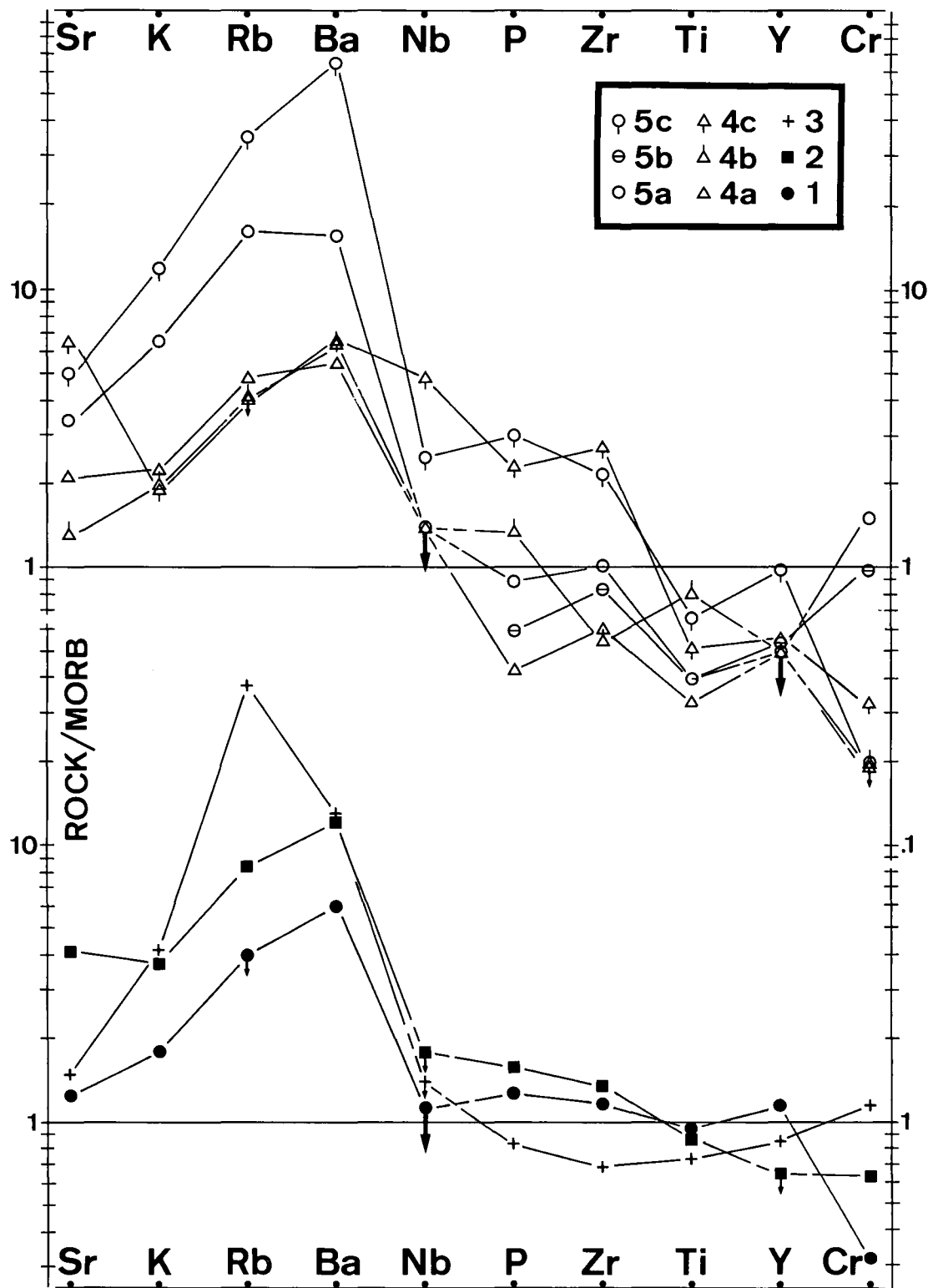


Fig. 8: MORB-normalised diagram for basalts and basaltic andesites after PEARCE et al. (1981). Values for MORB are: Sr 120 ppm, K<sub>2</sub>O 0.15 %, Rb 2 ppm, Ba 20 ppm, Nb 3.5 ppm, P<sub>2</sub>O<sub>5</sub> 0.12 %, Zr 90 ppm, TiO<sub>2</sub> 1.5 ppm, Y 30 ppm, Cr 250 ppm. Symbols as in Fig. 6. 5b = sample R3 which is considered to represent best the original element abundances (shown for P-Cr). Arrows indicate that part of the samples is below detection limit, bold arrows indicate that nearly all or all samples are below detection limit. Note the relatively flat patterns of elements with high ionic potential in the Basis Amphibolite; the depletion in these elements of "chemically unmodified" Weinbühel and Tauernkogel Amphibolites; the secondary enrichment in these elements in the "chemically modified" rocks. Note also the enrichment in low ionic potential (LIL) elements of all sequences; stronger enrichment of these elements in the Tauernkogel rocks is considered to be due to metasomatic influence from the intrusive Zentralgneis.

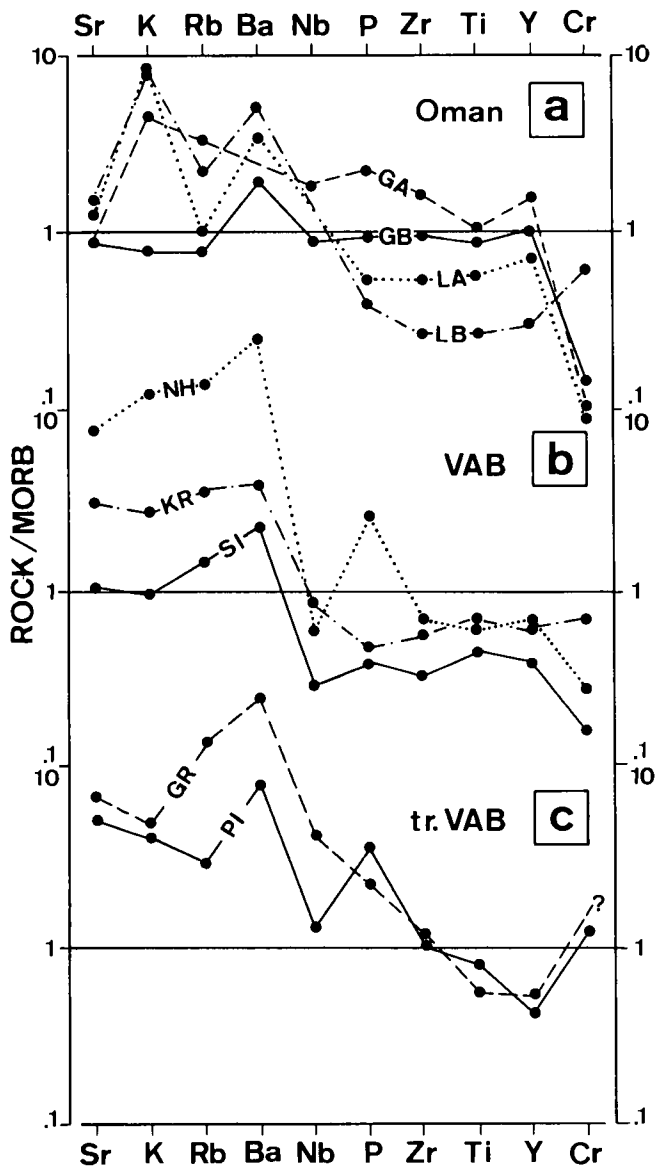


Fig. 9: MORB-normalised plots for comparison with basaltic rocks from different tectonic settings (PEARCE et al., 1981; PEARCE, 1982).  
 a: Oman ophiolite complex. GB = Geotimes Unit basalts; GA = Geotimes Unit basaltic andesites; LB = Lasail Unit basalts; LB = Lasail Unit basaltic andesites. Geotimes Unit is interpreted as back-arc sequence, Lasail Unit as island-arc tholeiitic sequence.  
 b: Volcanic arc basalts. SI = South Sandwich island-arc tholeiite series; KR = Krakatoa intermediate series (IAT/CAB); NH = New Hebrides high-K calc-alkaline series.  
 c: Transitional volcanic arc basalts comprising an alkaline component. PI = Penguin Island (South Shetland Islands); GR = Grenada (Lesser Antilles).

### 4.3. The Felbertal Mine Amphibolites

The amphibolites of the Felbertal scheelite mine, west field, are considered by HÖLL (1975) to be part of the Habach Formation. However, the amphibolites sampled from levels 1175 to 1188 are in average more mafic and chemically resemble the Basis Amphibolite. They contain high proportions of biotite when acid intrusives are close by. Coarse grained varieties may represent gabbroic source rocks.

The analysed rocks from the mine are all basaltic in composition (Fig. 6). The alumina content is lower than in typical calcalkaline rocks but there is no tholeiitic

character according to the iron content or the iron/magnesia ratio (Fig. 7). In the MORB normalised diagram (Fig. 8) the rocks show a clear arc character. The emplacement of granitic intrusives in the vicinity is suggested to be responsible for the stronger enrichment in K and Rb in comparison to the Weinbühel Amphibolite (such a relationship will be established with the Tauernkogel Amphibolites; see section 4.5.). The slightly abnormal pattern for trace elements with high ionic potential (relatively high Y and high Cr abundances) may have been caused by the ore forming processes. The scheelite deposit is considered to be of submarine-exhalative origin (HÖLL, 1975). On the other hand, back arc settings may produce similar patterns (PEARCE et al., 1981) when Cr is not fractionated and partial melting was less than in arc volcanics but slightly more than in N-type MORB. This interpretation is preferred here.

In the  $TiO_2$ -Zr diagram (Fig. 10) the Felbertal mine amphibolites are clearly separated from the Stubachtal and Basis Amphibolites and preferentially lie on the "arc" side of the arc/axis dividing line for Oman (PEARCE et al., 1981). They plot close to the tholeiitic basaltic andesites from Weinbühel (see below). In the diagram in Fig. 11 they take an intermediate position between tholeiitic and calc-alkaline rocks but fit well into the MORB field. In the Ti-V diagram (Fig. 12) their position is intermediate between MORB and volcanic arc basalt and fits well with back-arc basalts. In the diagram in Fig. 13 an arc component is again evident. The Felbertal mine amphibolites cluster well and coincide with the Stubachtal amphibolites. In the diagrams in Figs. 14 and 15 they occupy the (N-type) MORB fields which also contain island arc basalts. Again there is a close relationship to the Stubachtal rocks.

The sampled Felbertal mine amphibolites are basaltic in composition and show an arc component, but an oceanic crust component is also conceivable. A back arc setting is considered to be the best explanation for the chemical character of these rocks. Chemically they more resemble the Basis Amphibolite than the rocks of the Habach Formation. They may be a transitional member between the back-arc and the island arc settings.

### 4.4. The Weinbühel Amphibolite

The Weinbühel Amphibolite of Weinbühel and Messelingkogel is mainly of andesitic composition. Rocks of basaltic silica content are rare (Fig. 6). The two samples containing less than 47 %  $SiO_2$  (Fig. 6) are characterised by silica loss and increase in immobile trace elements due to metamorphic differentiation in shear horizons as exemplified above (Section 4.2.). Three samples from Messelingkogel containing between 65 and 70 % silica are extremely rich in plagioclase blastesis and contain a few percent mobilised quartz. It is therefore suggested that these were originally more basic in composition. The other three samples containing between 65 and 70 % silica (Fig. 6) contain in the order of 10–15 % mobilised quartz in veins, and therefore have an originally andesitic composition. In the AFM diagram (Fig. 7) these three samples, together with a group of three samples having silica contents of basaltic andesites, display a marked tholeiitic trend, which is confirmed by high  $FeO^*$  and low  $Al_2O_3$  (only in



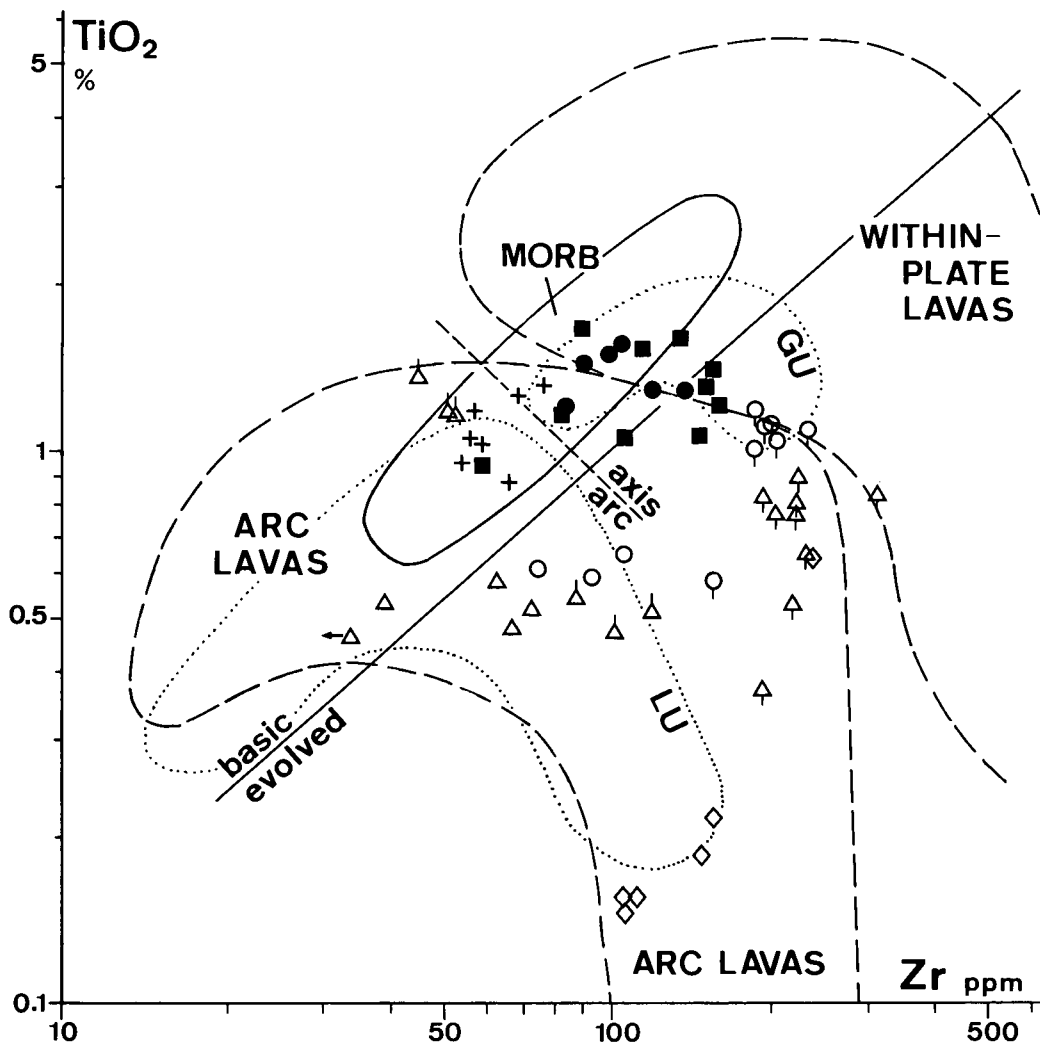


Fig. 10: Diagram after PEARCE & NORRY (1979) and PEARCE et al. (1981) for the discrimination of volcanic series. Symbols as in Fig. 6. MORB = mid-ocean ridge basalt field. Full straight line separates basaltic ("basic") and differentiated ("evolved") rocks. Dashed straight line separates back-arc ("axis") and island arc ("arc") series in Oman (PEARCE et al., 1981). Shown are also the fields for the Geotimes Unit (GU) and Lasail Unit (LU) in Oman. Note that most of the Basis Amphibolite samples plot on the "axis" side, and the "chemically unmodified" Weinbühel and Tauernkogel Amphibolites on the "arc" side. The "chemically modified" rocks plot close to the within-plate lavas boundary because of their passive enrichment in Ti and Zr due to strong deformation and recrystallisation. Note also the more basic (basaltic) composition of Basis Amphibolite in comparison with the more evolved Weinbühel and Tauernkogel rocks. The Felbertal mine amphibolites plot close to the Basis Amphibolites. The volcano-detrital rocks are again shown ( $\diamond$ ).

the latter group) values (Fig. 6). A distinct low-K character is evident in the  $K_2O$  diagram. Note the special symbols for the tholeiitic rocks in the diagrams.

The MORB normalised diagram (Fig. 8) shows enrichment in elements with low ionic potential and depletion of those with high ionic potential for those basaltic and basaltic andesitic rocks ( $SiO_2$  up to 57 %) whose original element abundances are thought (upon thin section study) to have been preserved ("chemically unmodified" rocks, symbols 4a and 4b). This pattern is typical of volcanic arc basalts (Figs. 9a and b [PEARCE, 1982]). Note that Nb and Y are below the detection limit in nearly all cases so that the plot gives a maximum value. Like in most other diagrams, the tholeiitic rocks of the Weinbühel sequence are different from the back-arc basalts of the Basis Amphibolite. The "chemically modified" samples, which underwent strong deformation and recrystallisation, have strongly elevated abundances in most elements with high ionic potential which have high stability in aqueous (metamorphic) fluids. The element pattern of this rock group resembles that of transitional volcanic arc basalts as they appear in specific arc settings and comprise an alkaline compo-

nent (Fig. 9c [PEARCE, 1982]). The petrographic survey of the samples and the low-K character, however, speak against such an interpretation.

In the  $TiO_2$ -Zr diagram (Fig. 10) the arc character is clearly displayed for the "unmodified" rocks. The shift towards higher Ti and Zr values for the "modified" rocks brings them close to or even into the within-plate field. The great part of the samples plot in this part of the "evolved" field, in which andesites should be located. In the diagram in Fig. 11 the stronger calc-alkaline character in comparison with the Basis Amphibolite is revealed. Only the three basaltic andesites already discriminated as tholeiitic plot into the tholeiite field. The "chemically modified" samples show a stronger but distorted calc-alkaline character. The same is true for the AFM diagram (Fig. 7). The volcanic arc character is confirmed in the Ti-V diagram (Fig. 12). Both basalts and basaltic andesites have been plotted in the diagram in Fig. 13. The "unmodified" non-tholeiitic rocks show a stronger calc-alkaline component than the rocks described hitherto. The tholeiitic samples plot as island-arc tholeiites. The "chemically modified" samples strongly shift towards the P corner. This is inter-

preted in terms of passive enrichment of the immobile mineral phase apatite during metamorphism. A slight shift in the Ti/Mn ratio in favour of Ti is considered to be due to a slight passive enrichment of rutile or sphene during metamorphism, while Mn has a more mobile behaviour. The diagrams in Figs. 14 and 15 are not suitable for the Weinbühel Amphibolite rocks because for their mainly andesitic compositions and their Nb and Y concentrations below the detection limit in most cases.

The great part of the amphibolite rocks of the Weinbühel Complex derived from andesites. Most of the primary rocks are believed to be low-K basaltic andesites, but low-K basalts and andesites are present as well. Most of the samples show a stronger calc-alkaline affinity as does the Basis Amphibolite, but some samples (derived from one or two horizons in the sequence) are markedly tholeiitic. The tholeiitic rocks are characterised by their abundance in modal garnet, and iron-rich hornblende (see Section 3).

#### 4.5. The Tauernkogel Amphibolite

The Tauernkogel Amphibolite is the same sequence as the Weinbühel Amphibolite but shows a marked

metasomatic influence by the intrusion of the Venediger Zentralgneis body. Zentralgneis tongues (e. g. Dichtenzunge, Fig. 1c, lower left) and aplite dike swarms penetrate the amphibolites of the Tauernkogel. The influence of the Zentralgneis becomes evident by biotite blastesis and, chemically, by strongly raised potassium contents (Fig. 6). Plagioclase blastesis and quartz mobilisation, moreover, indicate the unreliability of silica values. This is supported by the position of most samples with basaltic silica content on the evolved side of the dividing line in the  $TiO_2$ -Zr diagram (Fig. 10). The source rocks were probably the same as those of the Weinbühel Complex, i. e. mainly basaltic andesites.

The  $TiO_2$ -Zr diagram also suggests that only three samples contain their original trace element abundances, the other samples being shifted towards higher concentrations. This suggestion is supported by the microscopic and macroscopic survey of the samples, which exhibit evidence of stronger deformation. In the MORB normalised diagram (Fig. 8) all Tauernkogel samples have strongly raised K, Rb, and Ba abundances. The relationship with the intruding acid rocks is evident. The "chemically unmodified" amphibolites again show a tendency for depletion of elements with high ionic potential except for Cr, P, and Zr, which are

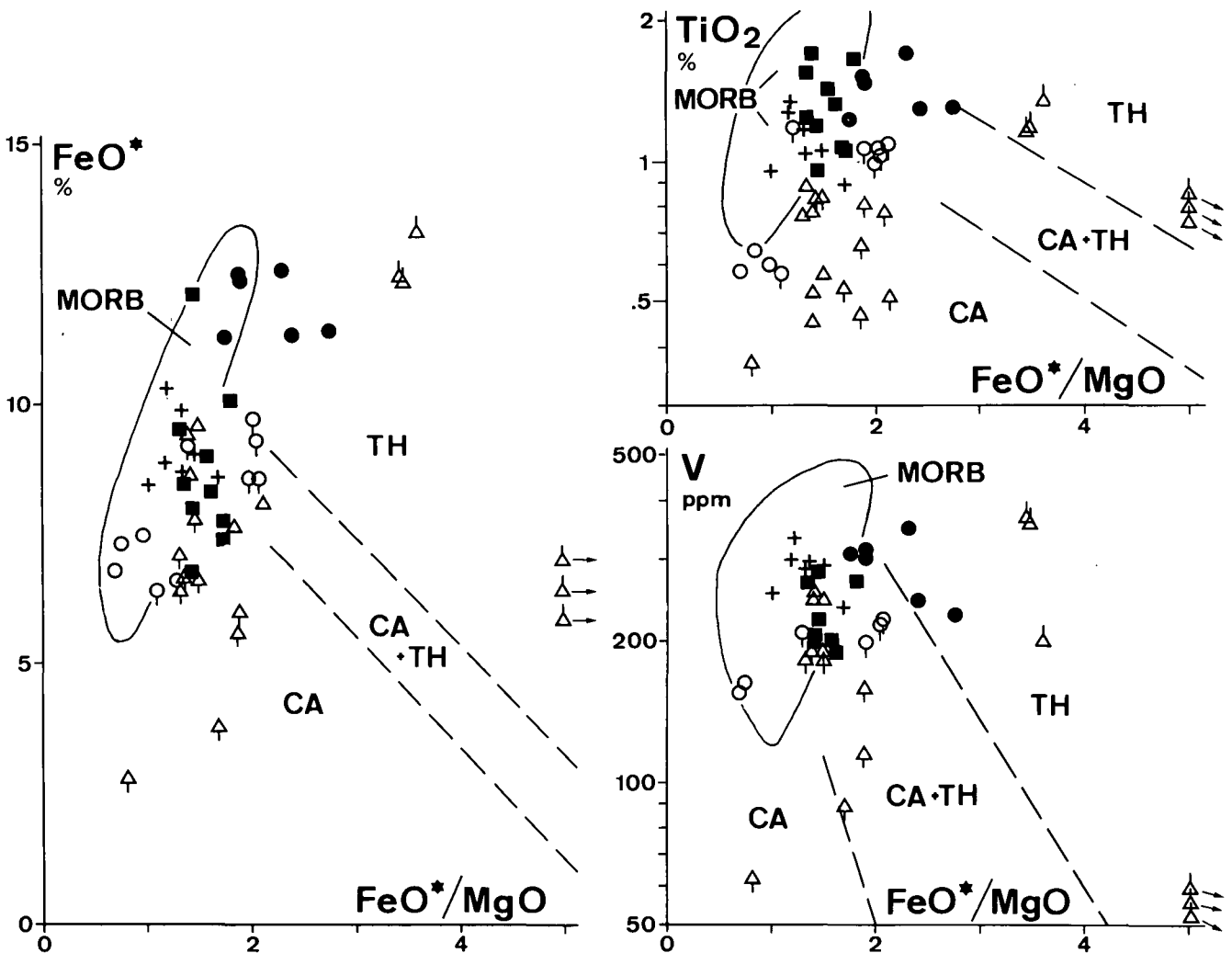


Fig. 11: Diagram after MYASHIRO & SHIDO (1975) for the discrimination of tholeiitic and calc-alkaline series. Symbols as in Fig. 6. Note the tholeiitic character of part of the Weinbühel Amphibolites and of the Stubachtal Amphibolites. Most other samples take an intermediate position. "Chemically modified" Weinbühel and Tauernkogel Amphibolites are shifted towards the calc-alkaline side.  $FeO^*$  is total iron.

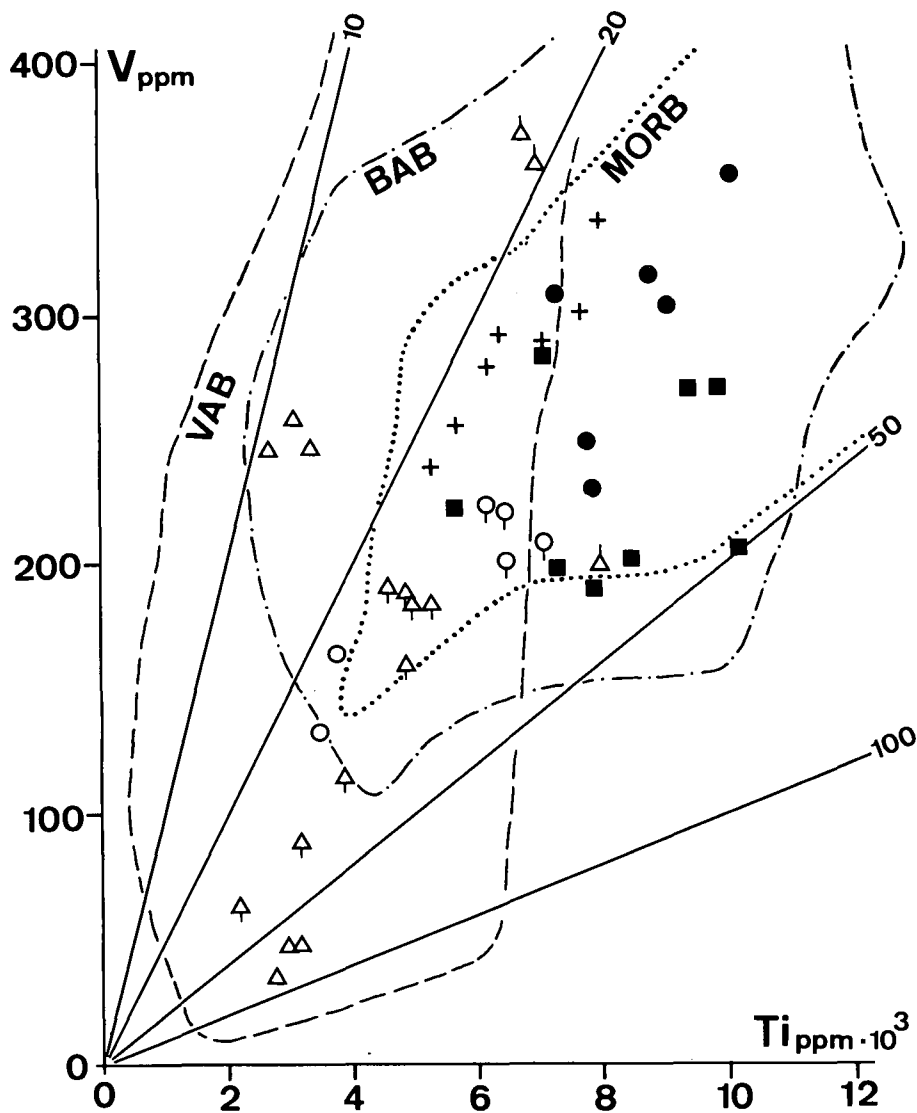


Fig. 12: Diagram after SHERVAIS (1982).  
 Shown are lines for different Ti/V ratios and fields for MORB = mid-ocean ridge basalts; BAB = back-arc basin basalts; VAB = volcanic arc basalts.  
 Symbols as in Fig. 6.

close to unity. The other samples are enriched in these elements relative to the "unmodified" rocks, except Cr. The different behaviour of Cr cannot be explained and may be due to local circumstances. The relatively high P and Zr abundances in the "chemically unmodified" rocks may indicate that these rocks were in fact subject to passive enrichment of these elements during deformation but to a lesser extent than the other samples. Sample R3 is considered to represent best the original composition of the rocks (symbol 5b in Fig. 8). In Fig. 13 it plots together with the "unmodified" Weinbühel Amphibolites and shows no secondary P enrichment. The stronger enrichment of the Tauernkogel rocks in elements with low ionic potential in comparison with the other groups (Fig. 8) is best explained in terms of granitoid metasomatism. The patterns for elements with high ionic potential in the Weinbühel and the Tauernkogel Amphibolites very much resemble each other for both the "unmodified" and "modified" rock groups.

In the diagrams in Figs. 10 and 13 the Tauernkogel Amphibolites behave like the Weinbühel Amphibolites. In the Ti-V diagram (Fig. 11) the "chemically modified"

samples take a marginal position to the volcanic arc field due to passive enrichment of Ti and V. In Figs. 7 and 11 the "unmodified" Tauernkogel rocks have a pronounced calc-alkaline character. The difference between these and the "unmodified" Weinbühel rocks may be explained by metasomatic variation in main element abundances.

In the diagrams in Figs. 14 and 15 the Tauernkogel samples take the position of volcanic arc basalts. Since the "chemically modified" samples plot into this field, the relative element proportions may have remained unchanged. The application of these diagrams is, however, problematic as we consider the original rocks to be basaltic andesites and not basalts.

The Tauernkogel Amphibolite is comparable to the Weinbühel Amphibolite and the same mode of origin, i.e. in an island arc setting, is proposed. The Tauernkogel Amphibolites, however, were subject to major changes in main and trace element concentrations by the influence of the Variscan granitoid and apatite intrusion and of Alpine deformation and metasomatism.

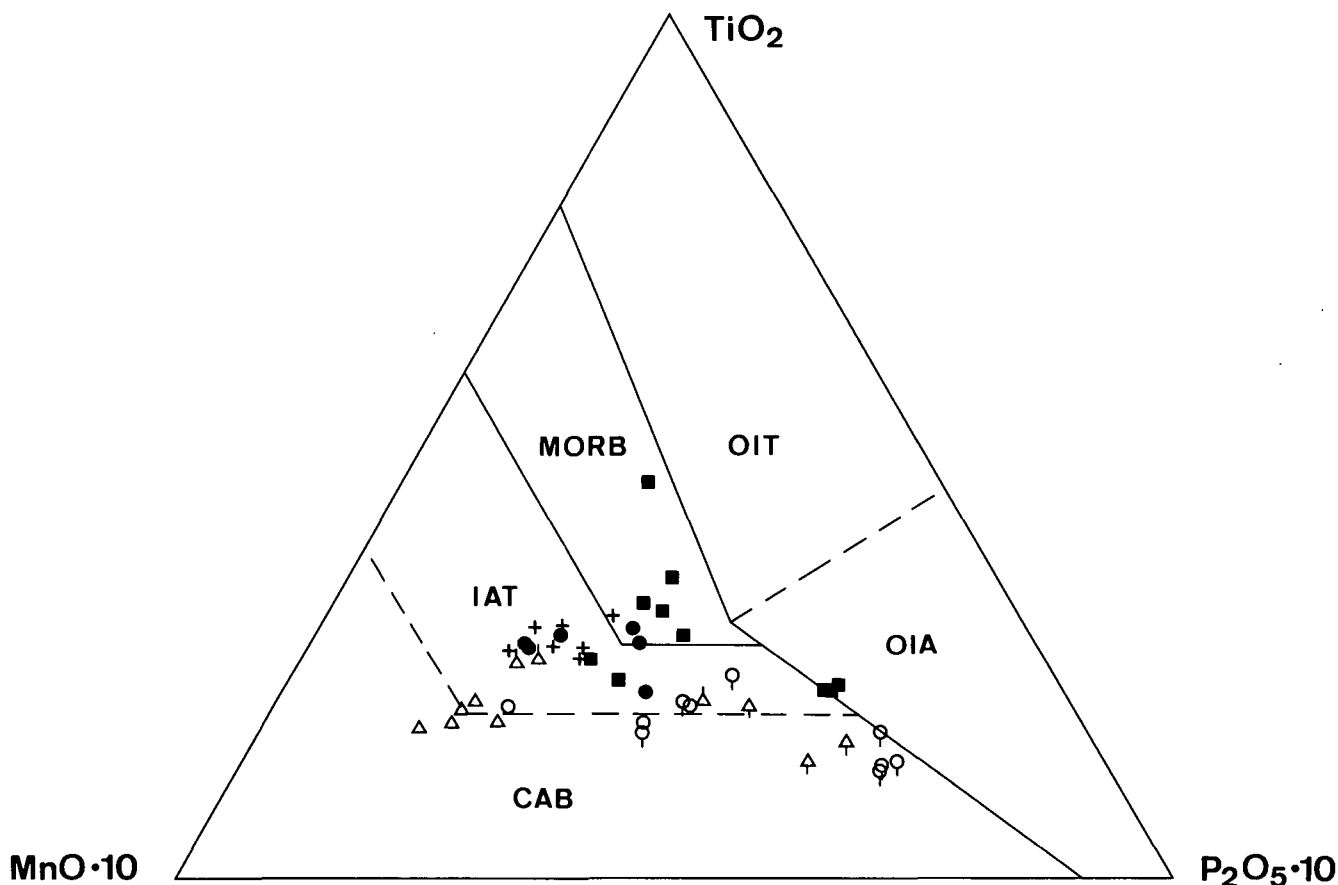


Fig. 13: Diagram after MULLEN (1983) for the discrimination of oceanic basaltic rocks. Included are amphibolite samples up to 57 % silica content. MORB = mid-ocean ridge basalt; IAT = island-arc tholeiite; CAB = calc-alkaline basalt; OIA, OIT = ocean island alkaline and tholeiitic basalt. Note the stronger calc-alkaline character of the non-tholeiitic Weinbühel and Tauernkogel Amphibolites and the tholeiitic character of the other series. Note also the shift of "chemically modified" Weinbühel and Tauernkogel Amphibolites towards the P corner due to passive enrichment of apatite during deformation.

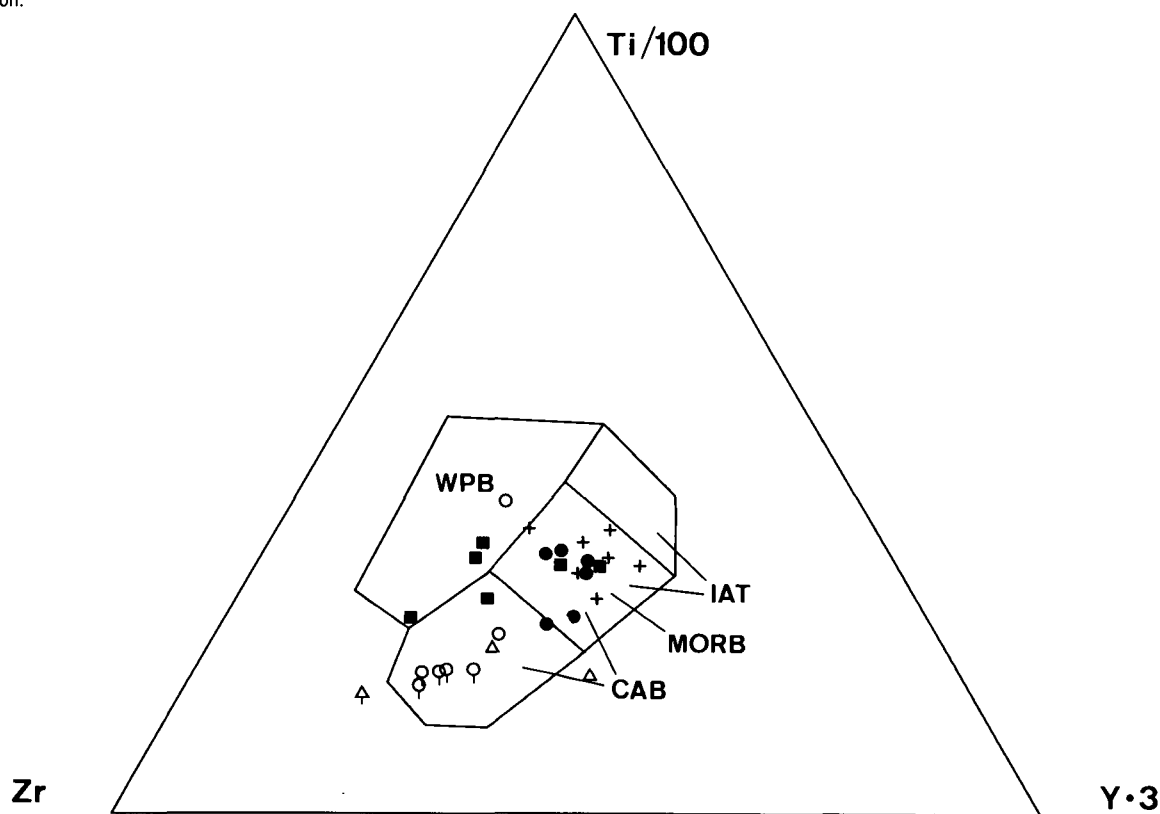


Fig. 14: Diagram after PEARCE & CANN (1973) for the discrimination of basaltic rocks. Symbols as in Fig. 6. Samples with Y abundance below the detection limit are not shown. WPB = within-plate basalts. Other abbreviations as in Fig. 13. Note the distinction between Basis plus Felbertal Amphibolites and Weinbühel-Tauernkogel Amphibolites.

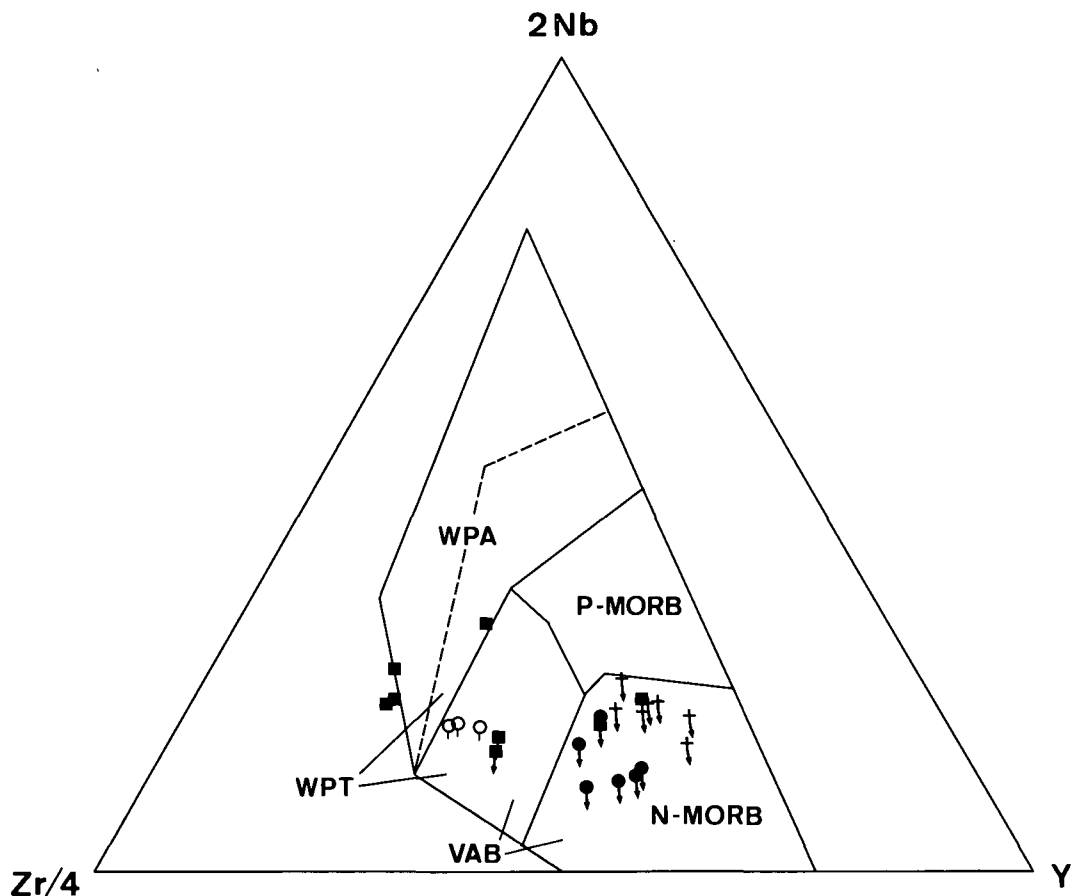


Fig. 15: Diagram after MESCHÉDE (1986) for the discrimination of basaltic rocks. Symbols as in Fig. 6. Samples with Nb concentrations below the detection limit are shown with arrows. WPA, WPT = within-plate alkaline and tholeiitic basalts; VAB = volcanic-arc basalts; P-MORB, N-MORB = enriched (plume related) and normal mid-ocean ridge basalts. Stubachtal and Felbertauern mine amphibolites are compatible with N-type MORB. Gabbroic Basis Amphibolite possibly contains a stronger volcanic arc component.

## 5. Discussion and Conclusions

The Penninic basement of the Venediger Nappe in the Tauern Window consists of two rock associations:

- 1) A sequence which is dominated by basic to intermediate volcanics in many parts (Habach Formation and equivalents [FRASL, 1958]) and
- 2) large granitoid masses which intruded into the first sequence.

Radiometric dating (v. QUADT, 1985) suggests that the metavolcanic series formed in the early Paleozoic which is in accordance with geologic evidence. The granitoid intrusions are late Paleozoic and were transformed into gneisses during the Alpine cycle (Zentralgneis).

Several amphibolite complexes have been investigated in the area between Granatspitz and Venediger Zentralgneis. The amphibolites represent metamorphic basalts and andesites. Acid gneisses are mainly of volcano-detrital or tuffitic origin. Non-volcanogenic metasediments (quartzites, impure marbles) are rare. Acid volcanics and graphitic schists are found in other areas (e. g. Habachtal [FRASL, 1958]).

In the investigated area Alpine metamorphism was prograde and of the medium-P type. The composition of zoned hornblende possibly suggests a slight decrease in the P/T ratio during metamorphic evolution. The amphiboles in the intercalated garnet amphibolites which display tholeiitic chemistry suggest higher pressures but since there is no indication for independent evolu-

tion of these rocks, the differences in mineral chemistry may better be explained in terms of the differences in rock chemistry. Alpine temperatures have attained about 550°C in the Basis Amphibolite east of Felbertauern. The medium-grade boundary is suspected to have been reached or slightly exceeded. Temperatures near the Tauernkogel summit are estimated to be somewhat lower, but they are still above the oligoclase isograd, i. e. above 500°C. In the other localities, maximum temperatures also have been in the interval between 500 and 550°C. The pressure is difficult to estimate but may be in the range of 5–6 kb at 550°C. No older metamorphic event is recognisable with certainty in the rocks investigated. Variscan hornblende (PESTAL, 1983), lawsonite pseudomorphs (early Alpine high-pressure event?; [FRISCH, 1984]) and, possibly, rutile relics (this study) point to earlier metamorphic events in several places.

The chemistry of the basaltic to andesitic amphibolites reveals two groups of rocks.

- 1) The Basis Amphibolite is mainly of basaltic composition. Ultramafic rocks and metagabbros are part of the succession.
- 2) The Weinbühel and Tauernkogel Amphibolites, which are separated by a major (probably pre-Alpidic) thrust plane, represent mainly metamorphosed basaltic andesites, but also andesites and basalts (Habach Formation). Basis Amphibolite and Habach Formation are also separated by a thrust plane.

The Basis Amphibolite succession consists of slices of an ophiolite sequence and represents ancient oceanic crust. The chemistry of the metagabbro and the meta-basalts, however, reveal a clear arc component, and therefore a back-arc tectonic setting is proposed for the formation of these rocks. They very much resemble the Geotimes unit of the Oman ophiolite complex, which is also interpreted as back arc oceanic crust (PEARCE et al., 1981).

The mainly andesitic sequence of the Weinbühel and Tauernkogel Complexes (Habach Formation) have low-K character and have been formed in an arc setting. The influence of magmatogenic aqueous fluids from the intruding Venediger granitoid in Variscan time changed the chemistry of the Tauernkogel rocks to high concentrations in K and other elements with low ionic potential. Moreover, where Alpine deformation was intense, it led to passive enrichment of immobile trace elements, in particular of P and Zr due to the stability of apatite and zircon. Nevertheless, the island arc character of the rocks can be well established.

The amphibolites of the Felbertal scheelite mine, which have basaltic composition, are considered by HÖLL (1975) to be part of the Habach Formation (Weinbühel sequence). Their chemical characteristics, however, are in contrast with those of the Weinbühel Amphibolites and in many respect resemble the basaltic Basis Amphibolite. It is therefore proposed that the basaltic amphibolites from the mine (levels 1175 and 1188) represent the transitional stage between back-arc setting and the superimposed island arc stage.

The low-K character of the arc suite (Habach Formation) and the association with mafic crust in a back-arc setting (Basis Amphibolite) raise the picture of a primitive island arc, which evolved on oceanic crust formed above the subduction zone in an earlier stage. During later orogeny the island arc sequence was tectonically sliced and thrust over the back-arc sequence. The image of a back-arc and primitive island arc environment is in contrast to the subduction related magmatism of roughly the same age in the Austroalpine Basement Complex (FRISCH et al., 1984 and in press). The much stronger emphasis on acidic rocks in the Austroalpine Basement Complex speaks in favour of an evolved island arc or an active continental margin setting. Therefore it is unlikely that the Penninic and the Austroalpine Basement Complexes formed in a continuous terrane in the early Paleozoic. The Rheic ocean between Africa and the North European craton was quite large at this time (SMITH et al., 1981), with enough room for several terranes with different structures. In any case, it is an area of crustal mobility, and several sites of subduction may have been active simultaneously (see also STILLE, 1980; PIN & LANCELOT, 1982). A similar situation existed in the late Proterozoic in northern Africa, where consolidation at the end of the Precambrian (Panafrikan cycle) forced crustal mobility to shift to the north. It may be speculated that the Austroalpine realm was located in the vicinity of the African continent, while the Penninic realm took an intra-oceanic position somewhere in the Rheic ocean.

The Variscan granitoids intruded some one hundred million years later into the mafic back-arc and island arc sequences. This was during the Variscan cycle which resulted in the cratonisation and consolidation of the region. The somewhat heretical question may be raised as to how far the greenstone-granite assemblage

of the Tauern Window resembles Archaean granite-greenstone belts. Although differences are to be expected as a matter of course due to the different thermal regime (komatiites!), the idea of a comparable tectonic setting of the rocks seems attractive. A back-arc setting of granite-greenstone belts has been repeatedly proposed. The general view, that the granites are younger in most cases is also in accordance with the Tauern Window situation. TARNEY et al. (1976) proposed a Tertiary example of back-arc setting in the Andes as a model for the Archaean greenstone belts.

#### Acknowledgements

The chemical analyses have been made by I. FETH, Geochemisches Zentrallabor, University of Tübingen. The microprobe analyses have been provided by Prof. P. METZ through D. MANGLIERS, Mineralogical Institute, University of Tübingen. Financial support was given from the Deutsche Forschungsgemeinschaft. Dr. P. WALSER, managing director of the Felbertal scheelite mine, and Dr. D. BRIEGLEB, chief geologist, enabled me to visit the mine and to take samples. Cand. geol. B. HASKELL corrected the English text. All this is gratefully acknowledged.

#### References

- BECKE, F.: Olivinfels und Antigoritserpentin aus dem Stubachtal (Hohe Tauern). – *Tschermaks Miner. Petr. Mitt.*, **14**, 271–276, Wien 1895.
- BRÖCKER, M.: Petrographische und geochemische Untersuchungen im Val Tuoi (Silvretta, Schweiz). – Unpubl. diploma thesis Univ. Tübingen, 108 pp., Tübingen 1985.
- BROWN, E. H.: The crossite content of Ca-amphibole as a guide to pressure of metamorphism. – *J. Petrol.*, **18**, 53–72, Oxford 1977.
- CORNELIUS, H. P.: Zur Geologie des oberen Felber und Matreier Tauerntals und zur Altersfrage der Tauernzentralgneise. – *Ber. Reichsst. Bodenforsch. Wien* **1941**, 14–20, Wien 1941.
- CORNELIUS, H. P. & CLAR, E.: Geologie des Großglocknergebietes. – *Abh. Zweigst. Wien Reichsst. f. Bodenf.*, **25/1**, 1–306, Wien 1939.
- DEER, W. A., HOWIE, R. A. & ZUSSMANN, J.: Rock forming minerals. Vol. 2: chain silicates. – 397 pp., London (Longmans, Green & Co.) 1963.
- EWART, E.: The mineralogy and petrology of Tertiary – Recent orogenic volcanic rocks: with special reference to the andesitic-basaltic compositional range. – In: THORPE, R. S.: *Andesites*, 25–95, Chichester (J. Wiley & Sons) 1982.
- FRASL, G.: Zur Seriengliederung der Schieferhülle in den mittleren Hohen Tauern. – *Jb. Geol. B.-A.*, **101**, 323–471, Wien 1958.
- FRASL, G. & FRANK, W.: Einführung in die Geologie und Petrographie des Penninikums im Tauernfenster (mit besonderer Berücksichtigung des Mittelabschnittes im Oberpinzgau, Land Salzburg). – *Der Aufschluß, Sonderh.* **15**, 30–58, Heidelberg 1966.
- FRISCH, W.: Geologie und Petrographie des Felbertauern-Straßentunnels (Osttirol). – *N. Jb. Geol. Paläont. Abh.*, **134**, 267–282, Stuttgart 1970.
- FRISCH, W.: Der alpidische Internbau der Venedigerdecke im westlichen Tauernfenster (Ostalpen). – *N. Jb. Geol. Paläont. Mh.*, **1977**, 675–696, Stuttgart 1977.
- FRISCH, W.: Tectonics of the western Tauern window. – *Mitt. Österr. Geol. Ges.*, **71/72**, 65–71, Wien 1980.
- FRISCH, W.: Metamorphic history and geochemistry of a low-grade amphibolite in the Kaserer formation (marginal Bündner Schiefer of the western Tauern Window, the Eastern Alps). – *Schweiz. mineral. petrogr. Mitt.*, **64**, 193–214, Zürich 1984.

- FRISCH, W., NEUBAUER, F. & SATIR, M.: Concepts of the evolution of the Austroalpine basement complex (Eastern Alps) during the Caledonian-Variscan cycle. – *Geol. Rundschau*, **73**, 47–68, Stuttgart 1984.
- FRISCH, W., NEUBAUER, F., BRÖCKER, M., BRÜCKMANN, W. & HAISS, N.: Interpretation of geochemical data from the Caledonian basement within the Austroalpine basement complex. – In: SASSI: Regional Volume, IGCP-Project No. 5, in press.
- FUCHS, G.: Beitrag zur Kenntnis der Geologie des Gebietes Granatspitze-Großvenediger (Hohe Tauern). – *Jb. Geol. B.-A.*, **101**, 201–248, Wien 1958.
- GRAHAM, C. M. & POWELL, R.: A garnet-hornblende geothermometer: calibration, testing, and application to the Pelona Schist, Southern California. – *J. Met-Geol.*, **2**, 13–31, Oxford 1984.
- HIETANEN, A.: Amphibole pairs, epidote minerals, chlorite, and plagioclase in metamorphic rocks, northern Sierra Nevada, California. – *Amer. Min.*, **59**, 22–40, Washington 1974.
- HÖLL, R.: Die Scheelitlagerstätte Felbertal und der Vergleich mit anderen Scheelitvorkommen in den Ostalpen. – *Bayer. Akad. Wiss., math.-naturw. Kl., Abh. N.F.*, **157**, 114 pp., München 1975.
- HÖLL, R. & MAUCHER, A.: The stratabound ore deposits in the Eastern Alps. – *Handbook of stratabound and stratiform ore deposits*, **5**, 1–30, Amsterdam (Elsevier) 1976.
- HOLLAND, T. J. B. & RICHARDSON, S. W.: Amphibole zonation in metabasites as a guide to the evolution of metamorphic conditions. – *Contrib. Mineral. Petrol.*, **70**, 143–148, Heidelberg 1979.
- LAIRD, J. & ALBEE, A. L.: Pressure, temperature, and time indicators in mafic schists: their application to reconstructing the polymetamorphic history of Vermont. – *Amer. J. Sci.*, **282**, 127–175, New Haven 1981.
- LEAKE, B. E.: The relationship between tetrahedral aluminium and the maximum possible octahedral aluminium in natural calciferous and subcalciferous amphiboles. – *Amer. Mineralogist*, **50**, 843–851, Washington 1965.
- LEAKE, B. E.: Nomenclature of amphiboles. – *Min. Mag.*, **42**, 533–563, London 1978.
- MESCHEDÉ, M.: A method of discriminating between different types of mid-ocean ridge basalts and continental tholeiites with the Nb-Zr-Y diagram. – *Chem. Geol.*, **56**, 207–218, Amsterdam 1986.
- MIYASHIRO, A.: Metamorphism and metamorphic belts. – 492 pp., London (George Allen & Unwin) 1973.
- MIYASHIRO, A. & SHIDO, F.: Tholeiitic and calc-alkalic series in relation to the behaviour of titanium, vanadium, chromium, and nickel. – *Amer. J. Sci.*, **275**, 265–277, New Haven 1975.
- MULLEN, E. D.: MnO/TiO<sub>2</sub>/P<sub>2</sub>O<sub>5</sub>: A minor element discriminant for basaltic rocks of oceanic environments and its implications for petrogenesis. – *Earth Planet. Sci. Lett.*, **62**, 53–62, Amsterdam 1983.
- PEARCE, J. A.: Trace element characteristics of lavas from destructive plate boundaries. – In: THORPE, R. S.: *Andesites*, 525–548, Chichester (J. Wiley & Sons) 1982.
- PEARCE, J. A. & CANN, J. R.: Tectonic setting of basic volcanic rocks determined using trace element analyses. – *Earth Planet. Sci. Lett.*, **19**, 290–300, Amsterdam 1973.
- PEARCE, J. A. & NORRY, M. J.: Petrogenetic implications of Ti, Zr, Y and Nb variations in volcanic rocks. – *Contrib. Mineral. Petrol.*, **69**, 33–47, Heidelberg 1979.
- PEARCE, J. A., ALABASTER, T., SHELTON, A. W. & SEARLE, M. P.: The Oman ophiolite as a Cretaceous arc-basin complex: evidence and implications. – *Phil. Trans. R. Soc. London* **A300**, 299–317, London 1981.
- PESTAL, G.: Beitrag zur Kenntnis der Geologie in den mittleren Hohen Tauern im Bereich des Amer- und des Felbertales (Pinzgau/Salzburg). – Unpubl. Ph.D. Thesis Univ. Vienna, 116 pp., Wien 1983.
- PETRAKAKIS, K.: Zur Geologie des Stubachtalultramafitit-Komplexes. – *Mitt. Ges. Geol. Bergbaustud. Österr.*, **24**, 47–57, Wien 1977.
- PIN, C. & LANCELOT, J.: Dating of an Early Paleozoic bimodal magmatism in the French Massif Central and its further metamorphic evolution. – *Contrib. Mineral. Petrol.*, **79**, 1–12, Heidelberg 1982.
- QUADT, A., v.: Isotope data from the scheelite deposit Felbertal (Eastern Alps) (abs.). – *Terra cognita*, **5**, p. 151, Strasbourg 1985.
- RAAB, D.: Genese der Amphibolitfolgen der alten Schieferhülle des Tauernfensters, Ostalpen. – Unpubl. Diploma Thesis Inst. Univ. Tübingen, 89 pp., Tübingen 1983.
- RAASE, P.: Al and Ti contents of hornblende, indicators of pressure and temperature of regional metamorphism. – *Contrib. Mineral. Petrol.*, **45**, 231–236, Heidelberg 1974.
- RINGWOOD, A. E.: Composition and petrology of the Earth's mantle. – 618 pp., New York etc. (McGraw Hill) 1975.
- SHERVAIS, J. W.: Ti-V plots and the petrogenesis of modern and ophiolitic lavas. – *Earth Planet. Sci. Lett.*, **59**, 101–118, Amsterdam 1982.
- SMITH, A. G., HURLEY, A. M. & BRIDEN, J. C.: Phanerozoic paleocontinental world maps. – 102 pp., Cambridge (Cambridge Univ. press) 1981.
- STEYRER, H. P.: Die Habachformation der Typlokalität zwischen äußerem Habachtal und Untersulzbachtal (Pinzgau/Salzburg). – *Mitt. Österr. Geol. Ges.*, **76**, 69–100, Wien 1983.
- STILLE, P.: On the genesis of the amphibolites and hornblendefelses in the Berisal Complex (Simplon; Italy-Switzerland). – *Mem. Sci. Geol.*, **34**, 205–246, Padova 1981.
- TARNEY, J., DALZIEL, I. W. D. & DE WIT, M. J.: Marginal basin "Rocas Verdes" complex from S. Chile: A model for Archean greenstone belt formation. – In: WINDELY, B. F. (ed.): *The early history of the Earth*, 131–146, London – New York – Sydney – Toronto (John Wiley & Sons) 1976.
- WEINSCHEK, E.: Beiträge zur Petrographie der östlichen Zentralalpen, speziell des Großvenedigerstockes I. – *Abh. Bayer. Akad. Wiss., 2. Kl.*, **18**, 651–714, München 1894.
- WINKLER, H. G. F.: Petrogenesis of metamorphic rocks. – 5th ed., 348 pp., New York – Heidelberg – Berlin 1979.

Manuskript bei der Schriftleitung eingelangt am 5. Mai 1986.